UNIVERSITY OF NEVADA, RENO

Introduction to Quartz Resonator Based Electronic Oscillators and Development of Electronic Oscillators Using Inverted-Mesa Etched Quartz Resonators

A thesis submitted on partial fulfillment of the requirements for the degree of
MASTER OF SCIENCE IN ELECTRICAL ENGINEERING

By
Matthew B. Anthony

Thesis Advisor
Dr. Indira Chatterjee

August 2009

THE GRADUATE SCHOOL

We recommend that the thesis
prepared under our supervision by

MATTHEW B. ANTHONY

entitled

Introduction To Quartz Resonator Based Electronic Oscillators And Development Of Electronic Oscillators Using Inverted-Mesa Etched Quartz Resonators

be accepted in partial fulfillment of the
requirements for the degree of

MASTER OF SCIENCE

Indira Chatterjee, Ph.D., Advisor

Bruce P. Johnson, Ph.D., Committee Member

Scott Talbot, M.S., Committee Member

Ronald Phaneuf, Ph.D., Graduate School Representative

Marsha H. Read, Ph. D., Associate Dean, Graduate School

August, 2009

ABSTRACT

The current work is primarily focused on the topic of the advancement of low phase noise and low jitter quartz crystal based electronic oscillators to frequencies beyond those presently available using quartz resonators that are manufactured using the traditional method that processes the entire sample to a uniform thickness. The method of inverted-mesa etching allows the resonant part of the quartz sample to be made much thinner than the remainder of the sample – enabling higher resonant frequencies to be achieved. The current work will introduce and discuss the importance of phase noise and jitter in electronic oscillator applications such as wireless communication systems and sampled data systems. General oscillator and quartz resonator background will be provided to facilitate the understanding of the oscillator circuit used herein. The Two Transistor Butler Oscillator circuit is first shown to function using traditional quartz resonators and then using the new inverted-mesa etched quartz resonators without performance degradation. Ultimately, the oscillator is shown to function using a 356.875 MHz inverted-mesa etched 3rd overtone AT cut quartz resonator. It is, therefore, demonstrated that the inverted-mesa etched quartz resonator can be used in the same oscillator circuits that use the traditionally processed resonators and can enable the economical use of quartz crystal oscillators at frequencies above that which was possible prior to their development. Furthermore, the increase in frequency without requiring external multipliers shows that performance increases can be made at still higher frequencies, precipitating improvements in systems that were previously limited by existing levels of oscillator phase noise and jitter.

This work is dedicated to

the furtherance of the understanding of God's wonderful created natural order,

the enthusiastic and diligent pursuit of excellence and righteousness in all things,

and my father William who taught me the importance of these two things.

ACKNOWLEDGEMENTS

Firstly, I would like to express my genuine loving gratitude to all my family, friends, and most especially my amazing wife for patiently allowing me to take the time to pursue and complete the current work. Without their loving encouragement, this work would not have been accomplished.

I would also like to express my sincere gratitude to Mr. Matt Eiting, President and Engineering Manager and Mr. Scott Talbot, General Manager and Marketing Manager at EM Research Inc., for their inspiration and support in the completion of the current work and for the resources supplied by EM Research, Inc.

I would like to also especially thank my Bachelors & Masters of Science studies academic advisor, Dr. Indira Chatterjee for her patience, help, support, and extensive commitment of time towards the completion of my academic accomplishment.

Additionally, I would like to thank Dr. Bruce Johnson and Dr. Ronald Phaneuf for their willing and accommodating participation in my thesis committee. Their contribution to the completion of the current work is sincerely appreciated.

Generous educators such as Dr. Chatterjee, Dr. Johnson, Dr. Phaneuf, and many others are enabling human advancement well beyond their own individual means and lifetimes by investing in the instruction and edification of others. Theirs is the highest and noblest work, and it is upon this work that all future innovations depend.

TABLE OF CONTENTS

LIST OF TABLES

LIST OF FIGURES

CHAPTER 1
OSCILLATOR INTRODUCTION & THESIS MOTIVATION

Oscillation is a cyclical variation of some parameter between more than one state. Typically, the variation is with reference to an average or central value and is quantified with respect to a known variable such as time or temperature. The parameter can be nearly any measurable quantity such as position, its derivatives velocity and acceleration; material properties such as mass, strength, and elasticity; material state such as solid, liquid, or gaseous; or electromagnetic such as field strength and orientation or instantaneous potential or charge.

A fixed or variable mass on an elastic spring or a pendulum swinging on a static line are examples of oscillation in position (and its derivatives) with respect to time. Rotation of a generation turbine is a position oscillation which induces an oscillation in electromagnetic fields between permanent magnets on the oscillating turbine and nearby stationary magnets. The field oscillations are captured by windings of conductive wire where they induce oscillating electric potentials that are propagated to common electrical outlets as alternating current. AC power generation is one example of a fixed-frequency electronic oscillator.

While the low frequency oscillations of AC power are useful for household and industrial electrical appliances, higher frequency electronic oscillators are important for other applications and are critical components within many technologies. Communications (and communications jamming), radar, and digital clock synthesis are just a few applications dependent on electronic oscillators. Furthermore, the listed applications are all systems within which the electronic oscillator performance and

limitations translate directly into overall system performance and limitations. The optimization of system performance, therefore, becomes largely an issue of optimizing the performance of the system electronic oscillator(s). Similarly, varied requirements of different systems precipitate the optimization of different – often competing – parameters of the electronic oscillator(s). This has driven the development of the various types of electronic oscillators currently available.

One such critical oscillator[1] performance parameter is its stability – or its ability to precisely maintain the desired output frequency. An ideal oscillator would generate a spectrum appearing as a single delta function at the desired frequency that would remain absolutely stationary despite fluctuations in the oscillator load, power source, environmental operating conditions, or the passage of time. A real oscillator, however, will produce a strong output at the desired frequency, but will also produce spectral energy at other frequencies. Nonlinearities, limiting, various noise sources, modulations, changing environmental parameters, and aging of the physical components all deteriorate the ideal delta function spectrum into an actual oscillator output spectrum similar to that shown in Figure 1-1. This figure illustrates several spectral issues encountered when implementing an actual oscillator. Integer harmonics are present due to nonlinear limiting, self-mixing of the desired signal, and harmonic resonances of the resonant circuit. Discrete spurious signals are present largely due to modulation of the oscillator from inadequately mitigated unwanted signals with a discrete frequency spectrum such as the switching frequency of the oscillator's power supply or signals coupled from nearby circuitry. Similarly, phase noise is the broad skirt of spectral energy present around the

[1] Subsequently, it will be assumed that an electronic oscillator is implied when the term oscillator is used unless otherwise specified.

desired signal and is due to short-term random fluctuations in the output of the oscillator from narrowband and broadband noise sources.

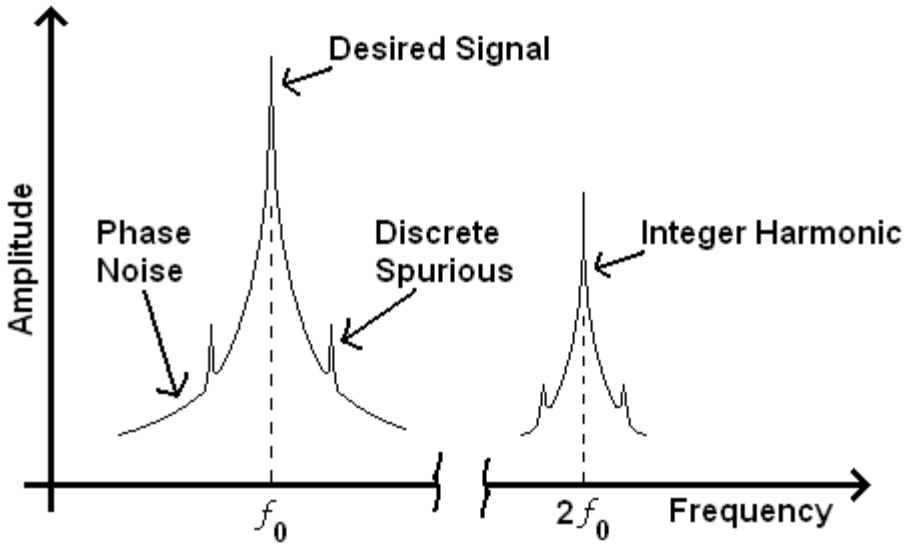

Figure 1-1: Oscillator Output Showing Deteriorations in the Ideal Spectrum

Being an octave or more separated from the desired signal, integer harmonics can be largely mitigated by conventional filtering techniques. The undesired spectral energy that is very close in frequency to the desired signal presents a more complicated problem as it cannot be easily filtered out using conventional techniques. The discrete spurious signals can be reduced or eliminated by reducing or eliminating the corresponding unwanted signals such as filtering power supply switching signals and isolating the oscillator from nearby circuits. The mitigation of the phase noise presents, generally, the most difficult design problem and can only be accomplished by selection of low-noise circuits and careful optimization.

It is widely known that oscillators based on quartz crystal resonators produce the purest spectral output (i.e. the lowest phase noise). As it has been traditionally

manufactured, the quartz resonator itself is limited in that it can only be constructed with resonance over a specific range of frequencies – up to around 230 MHz.

Therefore, the motivation for the current research project and thesis is to investigate the application of a new type of quartz resonator capable of frequencies higher than available using traditionally manufactured resonators. Increasing the range of the quartz resonator using the inverted-mesa etching process will allow low-noise quartz resonator based oscillators to be used at higher frequencies than previously available, improving performance in systems currently limited by existing levels of oscillator phase noise.

Chapter 2 will introduce more quantitatively the importance of oscillator phase noise using examples from two leading applications of frequency oscillators – wireless communication systems and sampled data systems. Chapters 3 and 4 will introduce some essential fundamentals of oscillators and quartz resonators respectively. Chapter 5 will introduce a specific oscillator circuit and show its performance in simulation and actual tests. Chapter 6 will then proceed to tuning of the oscillator to 200 MHz to show performance using a traditionally manufactured quartz resonator near the upper edge of the frequency range. Chapter 7 will proceed to the substitution of a 200 MHz inverted-mesa etched quartz resonator for the traditional example. The performance from a successful substitution will be compared with that from the traditional quartz resonator to ensure acceptable performance from the new resonator type. Finally, chapters 8 and 9 will again retune the oscillator to use an inverted-mesa etched quartz resonator above 350 MHz and conclude with a summary, discussion, and suggestions for future work.

CHAPTER 2
INFLUENCE OF PHASE NOISE ON SYSTEM PERFORMANCE

2.1 Wireless Communication Systems

Wireless communication systems are a specific application for oscillators that can be significantly influenced by oscillator phase noise. The oscillator implementation is typically as a fixed frequency or programmable Local Oscillator (LO) for the down and up conversion in superheterodyne receivers and transmitters. Phase noise is an instantaneous distortion in both phase and frequency, and, therefore, causes ambiguity in digitally modulated signals where phase and frequency increments are used to define different states. In this application, the phase noise generated by the oscillator will increase the probability of error or Bit Error Rate (BER) which represents the likelihood that any single received bit will not be received correctly. Pozar clearly shows that the BER associated with the detection of various digital modulation schemes is strongly associated with the overall noise content of a signal [1: chapters 8 & 9]. Higher BER slows down transmissions as the bit rate must be slowed down or information retransmitted additional times to compensate for the errors. Since noise and distortion generated by free space transmission is typically not controllable, the reduction in the noise added by the receiver and the transmitter are primary in the effort to keep overall noise to a minimum.

2.1.1 Quadrature Amplitude Modulation

A specific example of these effects on data rate and BER can be seen when examining the popular digital modulation scheme of Quadrature Amplitude Modulation

(QAM). QAM encodes raw data by modulating the amplitude of two carrier waves to a finite number of values. The two carrier waves are typically sinusoids and have a quadrature phase relationship (they are 90° out of phase with each other). One of the two carriers is defined as the in-phase signal (I) and may be a cosine waveform, leaving the other carrier to be defined as the quadrature-phase signal (Q) represented as a sine waveform.

In the United States, high data rate QAM modulation has been mandated for use in cable modem and digital cable television applications in standards developed by the Society of Cable Telecommunications Engineers (SCTE) which is accredited by the American National Standards Institute (ANSI) as an authority supporting the cable telecommunications industry [2].

In all digital modulation methods, each distinct state of modulation variable (phase, frequency, amplitude, etc.) encodes a unique pattern of raw binary bits known as a symbol. A larger number of distinct states allows more bits to be encoded per symbol. Generally speaking, if there are M distinct states or symbols in the modulation scheme, the number of binary bits N that can be encoded into each symbol is given by

$$N = \log_2(M) \qquad (2.1.1\text{-}1)$$

From equation 2.1.1-1, it becomes clear that only values of M that produce an integer value of N are efficient and practical. Alternately stated, since the raw data is binary, the number of combinations of finite modulation is optimized if they are powers of two (2, 4, 8, 16, 32, 64, 128, 256, etc.). Furthermore, in QAM, since the modulation is obtained by amplitude modulating two carriers, it is most logical to have each carrier modulate over the same scale and in the same finite increments. This further constrains the number of

symbols to values that are square (4, 16, 64, 256, etc). More symbols allow more bits to be transmitted at once, thus increasing bandwidth efficiency and data rates. For example, a QAM where M equals 16 means N equals 4, so four bits can be transmitted at once. Therefore, the data rate is four times the bit rate.

This is more easily understood when considering the constellation diagram for the modulation scheme. The constellation diagram is a visual representation of how the range of the modulation variable (amplitude in QAM) of the two carriers is divided into the finite number of combinations or symbols. The axes of the diagram correspond to the I and Q components mentioned earlier. The constellation diagram for a 16 symbol rectangular QAM (commonly abbreviated 16-QAM or QAM-16) is shown in Figure 2.1.1-1(a).

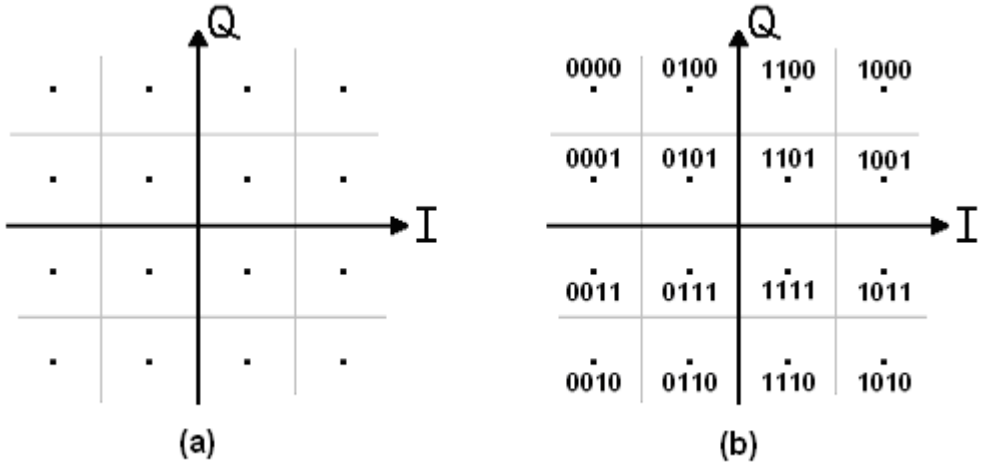

Figure 2.1.1-1: (a) Ideal 16-QAM Showing Perfectly Modulated Data in Each Symbol. (b) Ideal 16-QAM with Grey Code Bit Assignment to Available Symbols.

This figure shows the division of the modulation range of I and Q into 16 distinct symbols – each representing a specific combination of four binary bits. Generally, each symbol can be made to represent any specific combination of four bits, but in Figure

2.1.1-1(b), the bits have been assigned by means of the commonly used reflected binary code, also known as Grey code after Frank Grey the researcher who first described its use [3: page 51]. The advantage of the Grey code is that any two neighboring symbols represent a raw binary value that only differs by a single bit change which can facilitate error correction in digital communications.

Error correction is necessary because data transmitted using digital modulation is susceptible to corruption by many sources of noise and interference. Relevant to the current discussion is the influence of phase noise on the signal integrity of the QAM modulated data. Phase noise from the I/Q modulator, the heterodyne LO, and in-path transponders all contribute to disturb the accurate transmission of the modulated data. Since phase noise is a distortion in the frequency and phase of a signal, and is present in all frequency synthesizers to some degree, it will affect the quadrature relationship of the I and Q modulation carriers. The corruption of perfect quadrature of the modulating carriers can be seen as distortion of the data about the origin of the constellation diagram and is illustrated in Figure 2.1.1-2.

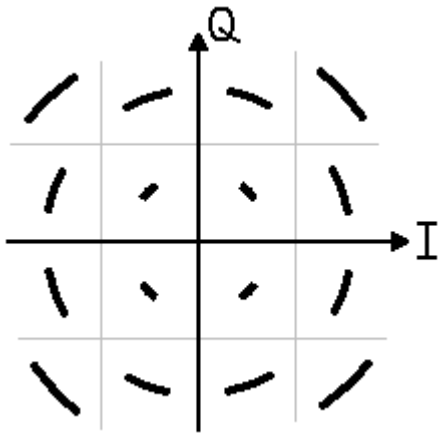

Figure 2.1.1-2: Distortion of the 16-QAM by Frequency Synthesizer Phase Noise

Rather than the ideal modulation shown in the earlier figure, Figure 2.1.1-2 clearly shows how imperfect carrier quadrature affects the demodulated data as it is interpreted much nearer to the symbol boundaries. Strictly speaking, in the presence of quadrature instabilities, the I and Q axes do not remain perfectly orthogonal. If one of the two axes is selected as the reference it will be considered stationary while the other will wobble back and forth around quadrature. It is this wobbling of one axis that is interpreted as a circular smearing of the demodulated modulation state. If the phase noise is too great, the demodulated data may be distorted to the degree that it crosses the boundary from one symbol into the next. This will result in the receiver demodulating the transmitted bits incorrectly. The signal will either need to be retransmitted or the data will continue on in a corrupted state. The success of retransmission is dependent on the BER being low enough for the signal to be received correctly much more often than it is received incorrectly. If the BER is unacceptably high due to phase noise that cannot be reduced, a simpler modulation scheme that uses less symbols or larger symbol boundaries

must be used. While decreasing the number of symbols when noise or distortion is very high may provide a net increase in data rate, it is by far better to be able to reduce the distortion and maintain the larger data rate afforded by having 16 symbols. Furthermore, it is even more desirable to increase the number of symbols to 64 or 256 for even faster data rates. Assuming relative signal amplitude maxima and minima remain the same, reductions in phase noise can make possible a 64-QAM or 256-QAM. A single quadrant of a 64-QAM constellation diagram including the effects of phase noise is shown in Figure 2.1.1-3.

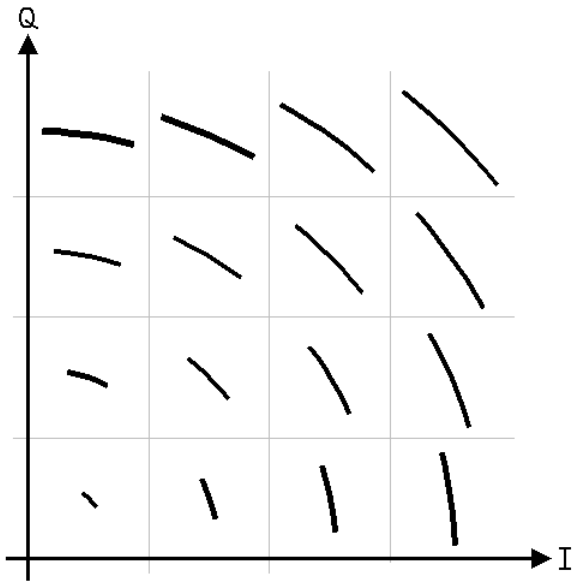

Figure 2.1.1-3: 64-QAM with Phase Noise Distortion

With 64-QAM and 256-QAM, the data rate can be increased to six and eight times the transmission rate (or baud rate) respectively. However, it should be noted that phase noise is not the only source of distortion acting on a communication system. Gaussian noise, AM, PM, and FM distortion (and others) all must be managed to maximize the number of available symbols and minimize BER to fully optimize the

available bandwidth and achieve the best possible net data rate. Also, while this explanation has been largely qualitative, the reader is referred to references [4], [5], and [6] for highly detailed explanations and calculations about how phase noise can influence BER, signal to noise ratio, and overall signal integrity in both QAM and other digital modulation methods.

2.1.2 Selectivity and Channel Spacing in RF Transmission

Phase noise can significantly degrade the selectivity of a wireless communications system [1: page 285, 7]. Selectivity is a figure of merit for a wireless communications system that represents its ability to select (receive in a receiver or transmit in a transmitter) a specific radio frequency (RF) communication channel while rejecting (not receiving in a receiver or not transmitting in a transmitter) the RF channels that are directly above and below. The narrow channel-spacing present in many wireless communication bands dictates that wireless receivers be constructed to have very narrow passbands, so that a single channel can be received without interference from neighboring channels. Take a standard FM band radio receiver, for example. Within this band, standard digital receivers can be tuned to channels spaced 200 kHz apart. While the Federal Communications Commission (FCC) regulates rights to a specific FM channel, the relative power level that any regional radio station uses to transmit its signal is more a budget issue as power amplifiers capable of transmitting increasingly stronger signals (allowing clearer reception over wider areas) and increasing electricity usage become very expensive. It is, therefore, not uncommon to have two adjacent FM radio stations transmitted at very different power levels. If the FM receiver being used has very good selectivity, however, the disparity in received signal strength between the two stations

will not cause a problem with receiving either one clearly. If the receiver selectivity is poor, however, the station with the higher transmitted power level may interfere with or entirely prevent the reception of the other.

While it may seem that the selectivity may be a parameter largely controlled by an input band-pass filter, highly selective tunable band pass filters are not at all simple to design and construct. Therefore, a wireless receiver front end may contain a band pass filter that passes the entire range of selectable bands (the entire FM radio band) on to a low noise amplifier (LNA). After the LNA, the signal is mixed with a tunable LO to down convert to an intermediate frequency (IF) or directly to baseband. Using a tunable LO allows the IF to be a fixed frequency. This means that a highly selective band pass filter can be designed around the IF which does not need to be tunable. If the conversion is directly to baseband, a selective low pass filter can be used instead. In either case, however, the signal has to be down converted (mixed) before the application of the selective filter. Since mixing is a convolution in the frequency domain, the presence of phase noise and discrete spurious signals in real oscillators can cause significant degradation in the selectivity of a wireless communications system. The phase noise of the LO within carrier offset frequencies of a megahertz or less can actually perform low-level down conversion of adjacent channels. This is made worse if an adjacent channel has much higher received signal strength than the desired channel. If the phase noise of the LO is high enough and the received signal strength is uneven enough, a weak station may no longer be detectable. This situation is illustrated in Figure 2.1.2-1.

When convolved in the frequency domain, the phase noise of the LO in Figure 2.1.2-1(a) creates a skirt about the higher power channel 2 from Figure 2.1.2-1(b) such

that the lower power signal at channel 1 is nearly lost. In Figure 2.1.2-1(c), channel 1 has paid the price of the degraded selectivity of the receiver – which is due to the phase noise of it's LO. This example effectively illustrates another danger oscillator phase noise can be to wireless communication systems.

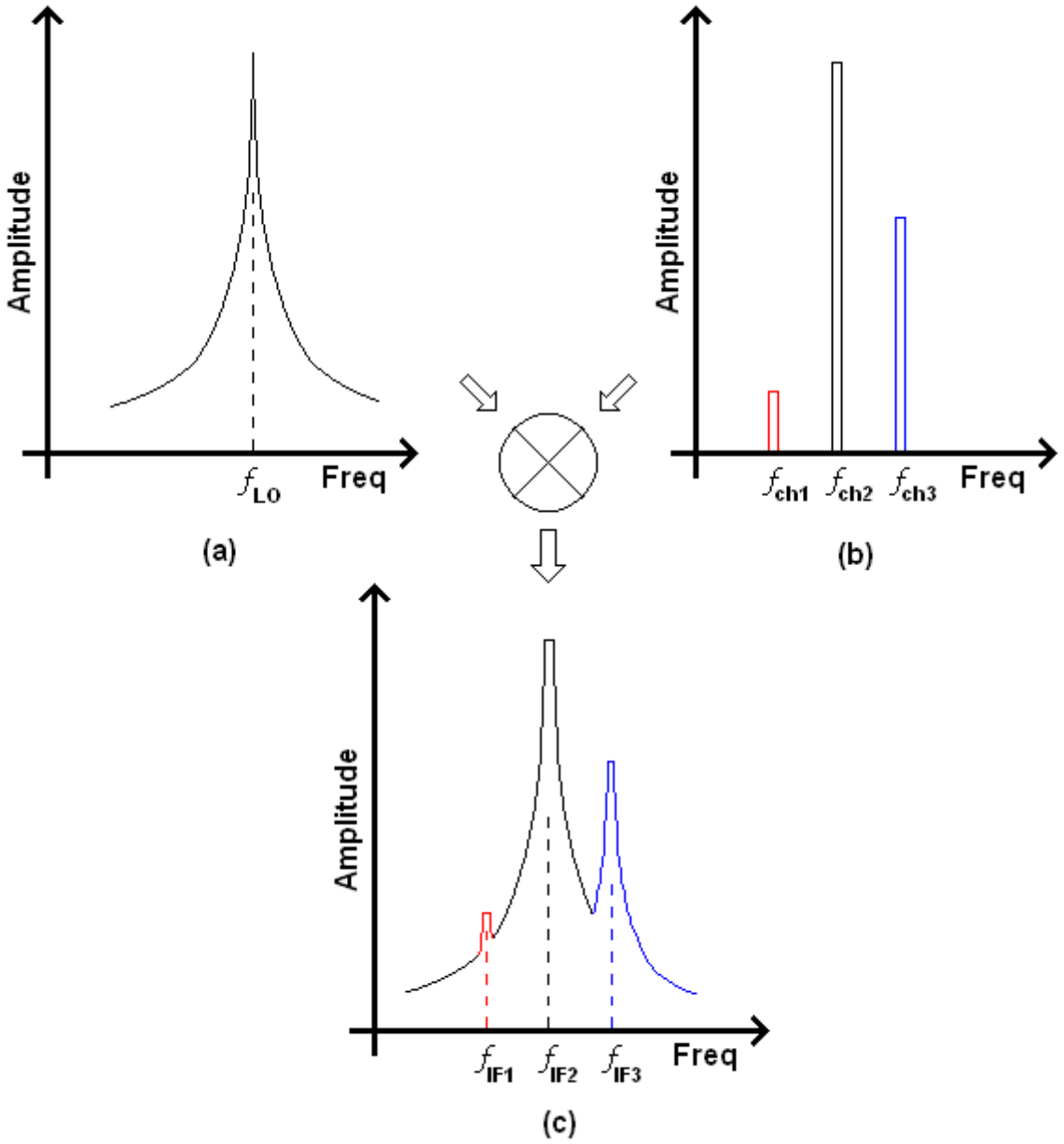

Figure 2.1.2-1: (a) LO with Phase Noise. (b) Spectrum of RF Channels. (c) Selectivity Failure Due to LO Phase Noise Convolved with RF Spectrum.

2.1.3 Bandwidth Efficiency

From sections 2.1.1 and 2.1.2, it is evident that the oscillator phase noise can degrade overall bandwidth efficiency in wireless communication systems. This degradation was seen as a reduction in the number of bits per symbol in QAM which forces a decrease in the available data rate. Decreasing data rate in the transmission means that less data is transmitted per unit time which is a decrease in bandwidth efficiency. Similarly, degradation in selectivity may necessitate larger channel spacings to maintain minimum received signal strength thresholds. Larger channel spacings mean that fewer channels can simultaneously occupy the RF spectrum. The RF spectrum is a finite resource and, as such, must be used as efficiently as possible. Increasing channel spacings to overcome hardware deficiencies such as phase noise limited selectivity results in further decrease in bandwidth efficiency.

2.2 High Speed Sampled Data System Sample Clocks

Sampled data systems are another specific application where oscillator phase noise can have a significant deleterious effect on system performance [8] - [14]. Sampled data systems include both analog to digital converters (ADCs) and digital to analog converters (DACs). Furthermore, these two systems are affected nearly identically by phase noise and its presence or mitigation. Knowing this, the current discussion will focus on the ADC for brevity.

Current wireless communication design trends are requiring ADCs to sample frequencies higher than ever before. Not only are they being used in baseband sampling where signal frequencies are less than or equal to half the frequency of the sample clock according to the well known Nyquist criterion [15], but higher frequencies are being

sampled that occupy higher Nyquist zones [16] which then become aliased onto the baseband – a process that is similar to and being used in place of analog heterodyning from the IF in a wireless receiver to the baseband. The RF signal is received by the antenna and down-converted to the first IF. This may be anywhere from 500 kHz to 250 MHz depending on the RF and LO being used. IF sampling simplifies the receiver architecture and allows for more advanced software defined radios (SDR). However, the ADC must now bear the burden of accurately sampling a much higher frequency analog signal than it did during traditional baseband sampling.

To understand the influence of phase noise on the ADC it is helpful to consider the transformation of phase noise into the time domain. The transformation of the short term phase and frequency instability known as phase noise into the time domain is known as time jitter. The skirt of energy shown as phase noise may be thought of as a probability distribution that the rising edge of the oscillator signal will actually occur at intervals given by exactly the period of oscillation. In Figure 2.3-1(a), a noiseless ideal oscillator spectrum translates to a perfect sine wave with zero crossings at exact intervals. In contrast, Figure 2.3-1(b) shows how the phase noise actually translates uncertainty to the time domain in the region where the zero crossings occur. The phase noise truly creates shifting or blurring of the sine wave along the time axis. This is shown as T_j, the time jitter and is quantified as an rms value. A method of calculating the approximate jitter from a phase noise distribution is presented very clearly in [17] and also in [8] and [12]. Alternately, the time jitter can be measured directly using advanced test equipment such as a spectrum analyzer or phase noise analyzer.

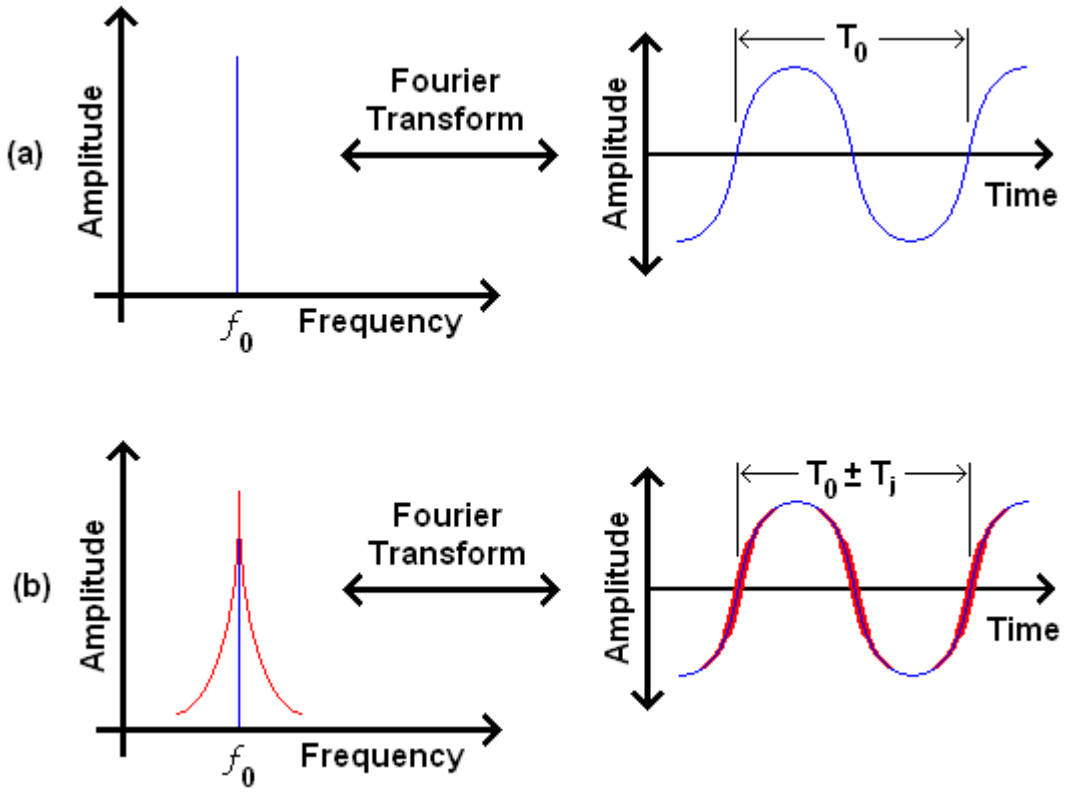

Figure 2.3-1: Ideal (a) and Real (b) Oscillators in the Frequency and Time Domains

The ADC process is literally driven by the oscillator being used as the sample clock (also called the encode clock). This clock (f_s) determines the instants in time at which the analog input signal (f_a) will be sampled or encoded. The jitter on the sample clock, therefore, introduces uncertainty in the sample acquisition time. This can be seen graphically in Figure 2.3-2(a) where the jitter in the sample clock (Δt) introduces an error (Δv) in the sample value of the analog voltage signal. The issue of increasing the frequency of the analog signal (f_a) is also illustrated in Figure 2.3-2(b) as the error increases significantly for the same sample clock jitter.

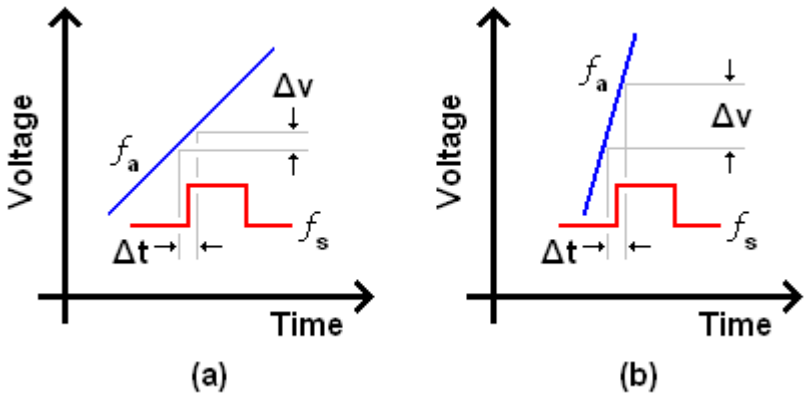

Figure 2.3-2: Sampling Error in Low (a) and High (b) Frequency Analog Signals

Slew rate is a figure of merit defining the speed at which a voltage waveform transitions from a minimum to maximum voltage or vice versa. In a digital circuit such as an ADC, events are triggered by signals passing predetermined voltage levels called threshold voltages which define the different digital levels of high and low – binary one and zero respectively. The sample clock in Figure 2.3-2 has been represented as a square wave because increasing the slew rate of the sample clock decreases the length of time spent near the threshold voltage of the ADC [12]. This is one way to help mitigate the distortion caused by the sample clock jitter and is accomplished by passing the sinusoidal signal from the oscillator through some type of signal conditioning circuit that increases the slew rate. Signal conditioning circuits, however, may contribute additional noise to the sample clock, so their selection and use must be performed with care. It should also be noted that the ADC itself has some jitter exactly when its sample and hold (or track and hold) amplifier (SHA) will record the sample – also known as the SHA aperture. So, even if the sample clock were totally ideal, there would be some sample error due to any active clock conditioning circuits (or clock distribution circuits) and the jitter of the SHA

aperture – this is illustrated in equation 2.3-1 where $t_{j,x}$ is the time jitter contribution of source x.

$$t_{j,total} = \sqrt{t^2_{j,\text{sample clock}} + t^2_{j,\text{clock conditioning}} + t^2_{j,\text{clock distribution}} + t^2_{j,\text{SHA aperture}} + \ldots} \qquad (2.3\text{-}1)$$

For IF sampled systems (or other high frequency sampled systems), the limitation on signal to noise ratio (SNR) from the time jitter can be determined by equation 2.3-2 [13] where f_a is the analog input frequency and $t_{j,total}$ is the total rms jitter contributing to aperture uncertainty in the ADC.

$$|\text{SNR}| = 20\log(2p\ f_a t_{j,total}) \qquad (2.3\text{-}2)$$

Using equation 2.3-2, a signal at 250 MHz being sampled by an ADC whose aperture has 1 ps of total time jitter will limit the SNR to only 56 dB. If the jitter could be reduced by a factor of two to 500 fs, the SNR would improve to about 62 dB.

From this analysis, it is clear that performance of high speed sampled data systems can quite easily be sample clock phase noise limited. Furthermore, as data continues to be sampled at ever increasing frequencies, the total jitter (phase noise) associated with the sample acquisition will need to be increasingly mitigated. Part of this mitigation is contingent on the design of the oscillator being used as the sample clock.

2.3 Phase Noise & System Performance Conclusion

Oscillator instability in the frequency domain (phase noise) and the time domain (jitter) significantly impacts overall system performance. The examples provided, wireless communication systems and sampled data systems, exhibit the importance of phase noise and jitter respectively on system performance. These systems (and others) would benefit significantly from the development of new, low noise oscillators.

CHAPTER 3
ELECTRONIC OSCILLATOR FUNDAMENTALS

3.1 Introduction

The electronic oscillator is an extremely complicated non-linear electronic circuit that can take many forms. When discussing a subject of such true complexity and with such a large existing body of knowledge, it is easy to become burdened with discussing minor details or explaining complicated models, equations, or derivations. Therefore, the following discussion will introduce some fundamental concepts required to understand all electronic oscillators without becoming too focused on one specific circuit topology. The use of equations and derivations will also be minimized for brevity. For a more thorough discussion including derivations and examples of multiple oscillator topologies the reader is referred to references [1: chapter 8, 18: chapter 12, 19: chapter 15, 20: chapter 7], or any other intermediate electronics textbook.

3.2 The Basic Electronic Oscillator

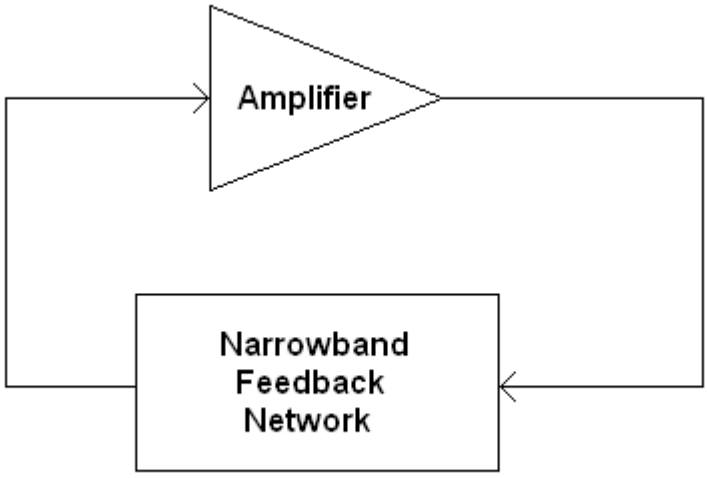

Figure 3.2-1: Basic Oscillator Model

The most basic model of an electronic oscillator consists of a circuit with positive gain such as an amplifier with its output connected to its input through some type of frequency selective feedback network as illustrated in Figure 3.2-1. The positive feedback at the selected frequency is passed to the input of the amplifier and hence receives gain or amplification. The amplified component again passes through the feedback network and receives additional gain the second time. In the ideal model above, this process would continue and the oscillations would increase infinitely. In a real circuit or system, however, the process will be limited by many non-linear factors and the oscillations will typically reach some steady state amplitude. This most basic model is surprisingly useful for describing a large number of working oscillator topologies – including the one that will be utilized in this project.

3.3 The Negative Resistance Model

Another important concept that aids in describing oscillations in electronic circuits is that of negative resistance. Consider an ideal inductor (L) and capacitor (C) connected in parallel. If energy is added to the circuit, it will oscillate back and forth between the two elements indefinitely. A real LC circuit will contain inherent parasitic resistances that make the circuit lossy. Energy added may oscillate back and forth initially between L and C, but will eventually fade and disappear. These situations are illustrated in Figure 3.3-1 (a) and (b). The energy added in (a) initiates sustaining oscillations. When the parasitic resistance is collected into an equivalent resistance R in (b), the added energy initially oscillates, but the oscillations are attenuated by the resistor each time the energy passes between the reactive components until they eventually stop completely.

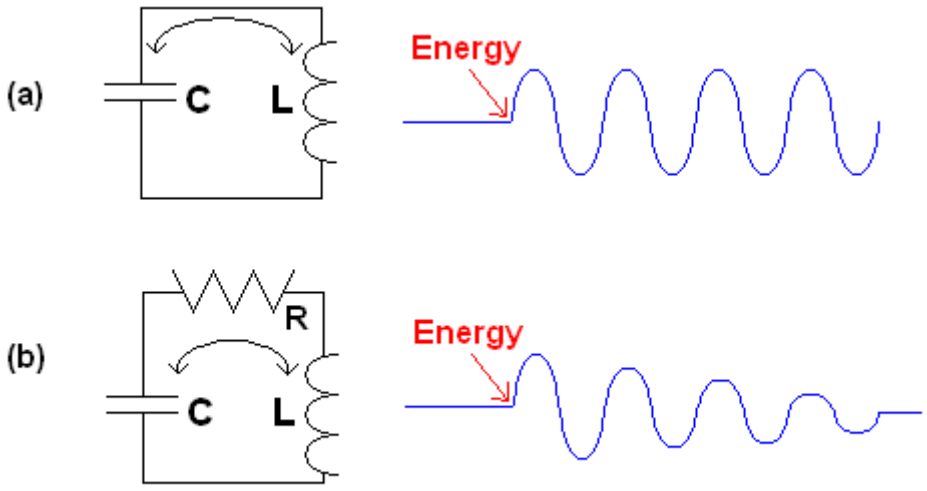

Figure 3.3-1: Added Energy Initiates Sustaining Oscillations in an Ideal System (a) and Decaying Oscillations in a Lossy Practical Circuit (b).

Suppose that another component could be added to the circuit that had resistance equal to R but opposite in magnitude – a negative resistance. If this were the case, the energy oscillating between the inductor and the capacitor would still be attenuated in each cycle by the lossy resistance R, but would be un-attenuated by the negative resistor –R. This is shown in Figure 3.3-2. Instead of dying out, the oscillations are sustained.

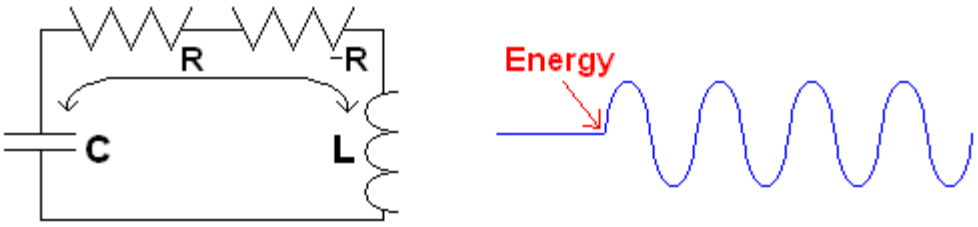

Figure 3.3-2: Added Energy Initiates Sustaining Oscillations in Lossy Practical Circuit with Negative Resistance

While a negative resistor may seem impractical, if the "un-attenuation" is instead thought of as gain, it then becomes apparent that the negative resistor is, in fact, an amplifier. The gain of this amplifier is exactly enough to counteract the attenuation of the parasitic resistance of the real inductor and capacitor. In this light, the circuit of Figure 3.3-2 is actually very similar to the basic oscillator model in Figure 3.2-1 – where the LC series circuit is the frequency selective feedback network and the negative resistance is a circuit with gain such as an amplifier.

Again, the active circuit (a transistor amplifier for example) will resupply an amount of energy equal to that which is being attenuated during each cycle of oscillation. A helpful analogy for understanding the negative resistance concept is an adult pushing a child on a swing. Without the adult's extra little push each cycle, the child's oscillations would eventually diminish and stop. The drag from air friction on the swinging child is analogous to the parasitic resistance in the circuit.

3.4 One Port Resonator Configuration

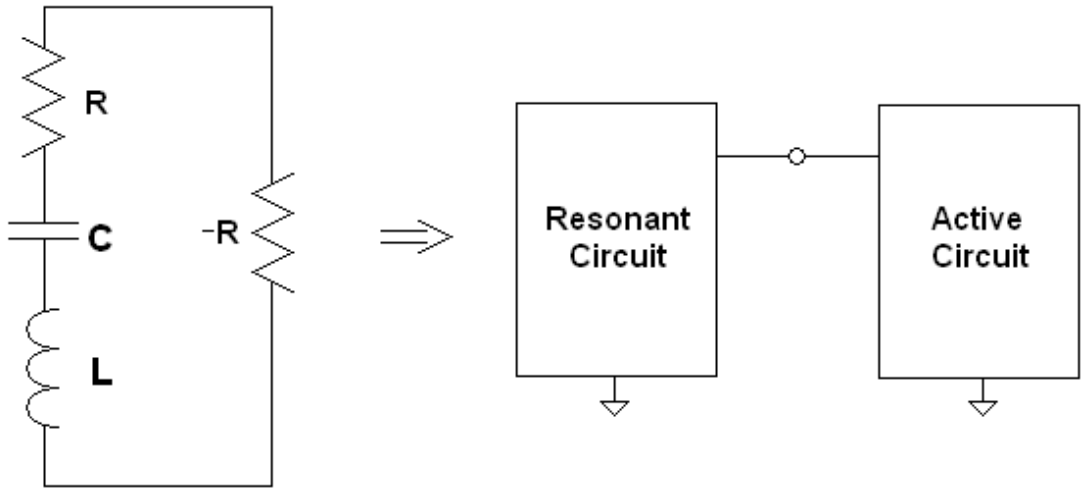

Figure 3.4-1: Reconfiguration to One-Port Circuits

In the last section, the circuit in Figure 3.3-2 was illustrated with the equivalent resistance and negative resistance between the reactive elements, but it should be noted that the simple series circuit can be rearranged as seen in Figure 3.4-1. The series reconfiguration leads to another practical oscillator configuration – one with a resonant circuit connected to an active circuit at a single active port and a reference point or ground point. Just as in the prior section, the active circuit resupplies whatever energy is lost by the parasitic resistance in the resonant circuit. This configuration is particularly useful as the resonator and active device can be subdivided into two one port networks. Each one can be analyzed via its one-port S-parameter S_{11}.

3.5.1 Quality Factor: Definitions and Implications

Whether a loop configuration (Figure 3.2-1 – 3.3-2) or a dual one-port configuration (Figure 3.4-1) is used, a critical figure of merit for a frequency selective (or resonant) circuit is quality factor (Q factor or simply Q). Several definitions for Q exist. A good physical interpretation of Q for a resonant circuit defines it as $2p$ times the ratio of energy stored to energy dissipated per oscillation and is shown in equation 3.5.1-1 [18: page 268],.

$$Q \equiv 2p \frac{\text{Energy stored during a cycle}}{\text{Energy dissipated per cycle}} \tag{3.5.1-1}$$

According to this definition, increasing Q indicates a decreased rate of energy dissipated during each cycle of oscillation. It is also intuitive from this definition that for Q to increase, the resonant circuit must be made less dissipative or less lossy. This implies a direct connection between increasing Q and decreasing parasitic resistance in the resonator. In fact, equation 3.5.1-2 shows the calculation of Q for a series RLC circuit and clearly shows the inverse relationship between R and Q [18: page 272].

$$Q = \frac{1}{R}\sqrt{\frac{L}{C}} \tag{3.5.1-2}$$

Another definition of Q for resonant circuits is the resonant frequency f_{res} divided by the half-power (-3dB) bandwidth (BW) of the resonator and is seen in equation 3.5.1-3 [18: page 269]. This equation reveals an important aspect of tuned circuits. As the circuits become less lossy (less resistive & more reactive) for a given resonant frequency, their bandwidth will decrease proportionately. Therefore, the resonator becomes more efficient at its center frequency and less efficient at surrounding frequencies.

$$Q = \frac{2p\ f_{res}}{BW} \tag{3.5.1-3}$$

3.5.2 Quality Factor: Connection to Practical Design and Phase Noise

Since resistance is parasitic in reactive components, selection of superior components can result in higher Q resonant circuits. This can become a function of material properties, manufacturing methods, physical component size, and cost. Additionally, consistency must be achieved on the part of the component manufacturer by careful understanding and control of the fabrication process and quality assurance testing.

Additionally, the resonator component Q is not the total oscillator circuit Q – also known as the loaded Q [18: page 271]. This factor is a complicated combination of the Q of each element in the oscillator and is dependent on the circuit topology and any circuits connected to the oscillator – such as active biasing, electronic tuning, and the tap point that draws a portion of the oscillating energy for external use.

One final implication of resonator Q that is particularly relevant to the current work is its connection to the phase noise of an oscillator. No simple equations exist defining general connections between resonator Q and phase noise, but examples in later chapters will demonstrate that higher Q oscillators produce less phase noise than lower Q oscillators. Furthermore, this connection also alludes to one of the primary concessions in oscillator design – bandwidth and phase noise performance. While not mutually exclusive due to the fact that Q is only one factor in the overall phase noise of an oscillator, they are, generally speaking, inversely proportional. Again, the relationships between Q, phase noise, and bandwidth will be clearly illustrated in later chapters using measured data from quartz resonators and functioning oscillators.

3.6 Electronic Frequency Control or Tuning

Another critical parameter for an oscillator is electronic frequency control (EFC) or electronic tuning. This may or may not be a specific requirement for every application, but, from a design perspective, the capability for an electronic circuit (like a microcontroller or microprocessor) to adjust the frequency output of the oscillator can be used for tuning to multiple channels in a communications band, for aging and/or temperature compensating frequency adjustments, and for phase/frequency locking the oscillator to another (usually more stable) oscillator in a phase locked loop. Adding EFC to an oscillator creates a voltage controlled oscillator (VCO) [1: page 258].

To make the oscillator tunable, a component with adjustable reactance must be added to the frequency selective or resonant circuit. While the inductive element can be made adjustable, it is much more common to vary the capacitance to achieve tunability. One method of accomplishing this is to use a voltage controlled capacitor such as a varactor. A varactor is simply a reverse-biased diode, whose pn junction doping profile has been optimized to create a specific and repeatable relationship between reverse-bias DC voltage and junction capacitance, or depletion layer capacitance [18: page 520-521, 19: page 22-23, 21].

The varactor is often used in series or parallel with a fixed value capacitor to provide tuning about a center frequency. Since the varactor must be DC biased, it is also necessary to include DC blocking capacitors to prevent the bias from influencing other elements and RF blocking elements to prevent detuning of the resonant circuit by the DC bias circuitry.

CHAPTER 4
THE QUARTZ RESONATOR

4.1 Qualitative Motivation for Quartz as a Resonant Element

Quartz is a tetrahedral lattice of silica (silicon dioxide) that occurs abundantly in the Earth's crust and possesses piezoelectric properties that help make it suitable for use as the frequency resonant element in an electronic oscillator. Additionally, pieces of quartz can be fabricated such that environmental temperature variations induce very little change in the resonant piezoelectric properties. Perhaps most importantly, many companies have been supplying quartz crystal resonators for many years leading to a very well understood and controllable manufacturing process that produces an inexpensive and consistent product [22].

Naturally occurring quartz is insufficient for use in an oscillator due to the presence of impurities within the crystal lattice. Impurities in the lattice will corrupt its piezoelectric continuity and frustrate the natural resonance of the sample. Therefore, the raw quartz crystal used to manufacture high quality electro-mechanical resonators is artificially grown under highly controlled conditions and is free of impurities. The manufactured quartz is naturally occurring impure quartz that is decrystallized in an autoclave and allowed to recrystallize without the original impurities [22].

Piezoelectricity is the ability of certain materials to generate an electric potential when a mechanical stress is applied. The stress disturbs the uniform charge distribution of the static material creating an electric potential across it. Conversely, the application of an electric potential or field will induce a mechanical deformation of the material. Additionally, the crystal lattice possesses natural resonant frequencies at which it will

mechanically oscillate with maximum amplitude. This resonant frequency depends on properties of the lattice, such as its purity, size, shape, and the manner in which it was cut with respect to the larger crystallographic lattice [23]. Therefore, if an electric field is applied to a sample of piezoelectric material that contains an energy component at its resonant frequency, the material will readily respond with an appropriate deformation.

While many materials possess piezoelectric properties, it is the combination of temperature stability, availability, and workability that make quartz such an attractive option for controlling the resonant frequency of an oscillator. While the raw material is a large, purified tetrahedral lattice of silica, the finished product used in a resonator is a small cut section mounted in a protective metal housing. The shape, size, and orientation in which the section is cut from the raw anisotropic lattice is particularly important as it will dictate not only the resonant frequency of the section, but its stability versus changing temperature and whether its mode of vibration is flexural, extensional, or shear – each of which additionally dictate many significant factors relevant to the use of the sample as a resonant element [24, 25].

While nearly infinite combinations of sample shape and orientation relative to the crystallographic axes exist, one very popular cut is known as the "AT" cut. The AT cut produces a sample whose mode of vibration is a thickness shear [26, 27] and can be fundamentally related to the thickness of the sample or related to one of the odd mechanical overtones of its fundamental mode. The thickness shear flexure for a fundamental mode (a) and a 3rd overtone (OT) mode (b) is illustrated in Figure 4.1-1. The instantaneous flexure of the lattice in the shear directions indicated by the blue arrows distorts the nominal shape of the sample to match the red outline. The sample thickness

dictates the wavelength of the half cycle (a) and full cycle (b) lattice shear distortions. From this, it can be seen that higher resonant frequencies are associated with decreasing thicknesses of the sample. Above a resonant frequency of around 45 MHz, the sample thickness becomes so small that the sample is too fragile and can no longer be processed using traditional cutting and grinding methods [28]. For higher frequencies, it is necessary that the sample thickness be increased and the resonance be made to occur at one of the odd mechanical OTs. The mechanical OTs of the sample are generally not exact harmonic multiples of the fundamental frequency – which is why it is important to define the resonant frequency and the desired OT when specifying a quartz resonator [20: page 30, 28]. Furthermore, if oscillation on an OT is required, another tuned circuit must be present in the oscillator design to suppress fundamental or lower OT oscillations.

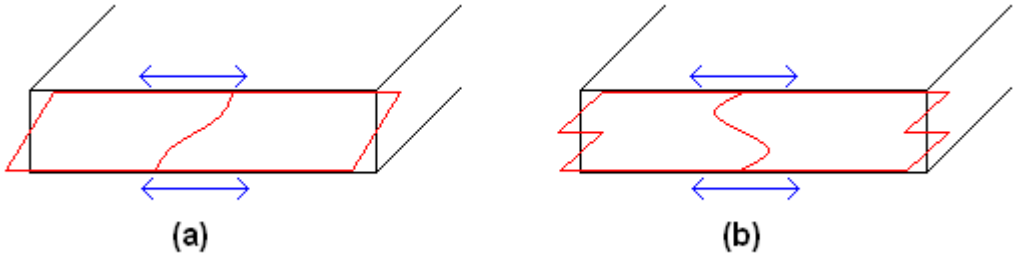

Figure 4.1-1: Thickness Shear Mode Fundamental (a) and 3rd OT (b)

Once cutting and other preparations are complete on the AT cut sample or wafer, electrodes are applied to the opposite sides of the wafer by deposition or photolithography. The electrodes are then connected to leads that can be connected to a circuit board while the wafer is retained between clips that prevent contact with the inside of the protective housing. The assembly is typically mounted inside a hermetically sealed metal housing to prevent contaminating materials from collecting on the wafer and

changing the resonant frequency or behavior. The metal housing is constructed so that the leads extend out or connect to terminations that are transferred to the outside for connection in an electronic circuit. Figure 4.1-2 shows a sealed resonator (a) with protruding leads and (b) where the protective housing has been removed – revealing the quartz wafer with the deposited electrodes on either side and the metal clips which contact the electrodes and transfer the connection to the leads that extend through the base at the bottom for circuit connection.

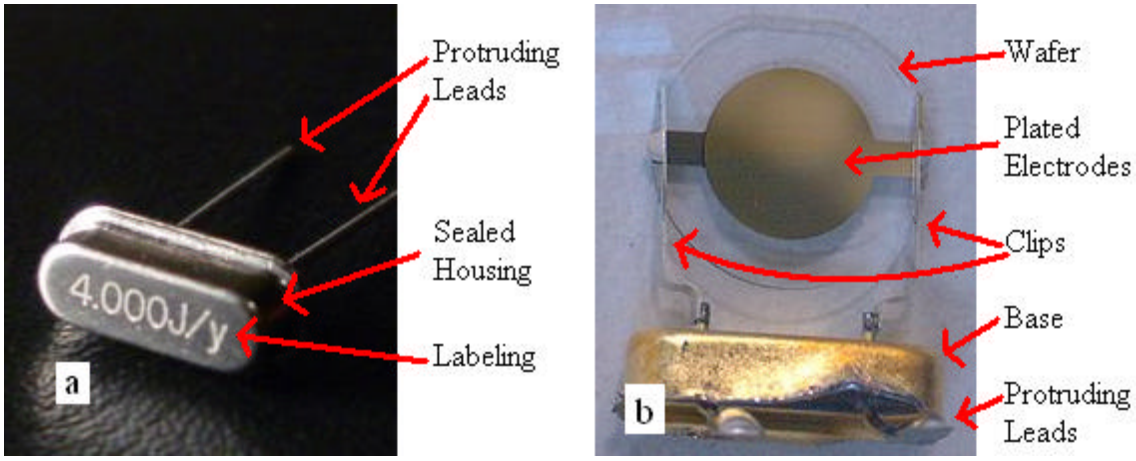

Figure 4.1-2: Mounted Resonators with Cover In-Place (a) and Removed (b) [29]

4.2 Quantitative Motivation for Quartz as a Resonant Element

The quantitative analysis of the quartz resonator facilitates a clear understanding of when and why it is used in electronic oscillators. The following sections will introduce and discuss the equivalent circuit for a quartz resonator. Measured data from several units will also be presented along with plots of the equivalent impedance of the quartz resonator. Several figures of merit will be introduced that are relevant to the specification of a quartz resonator for use in oscillator applications. The benefits of the use of the quartz resonator will be discussed as well as its minor and major limitations.

4.2.1 Circuit Symbol & Basic Equivalent Circuit

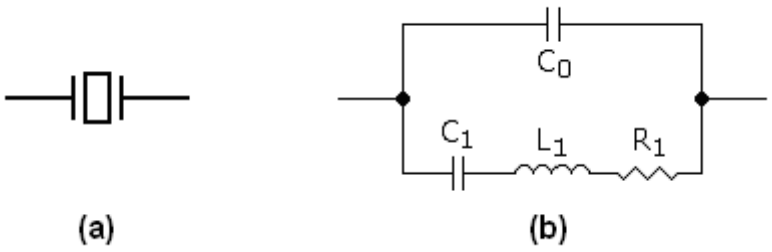

Figure 4.2.1-1: Quartz Resonator Symbol (a) & Basic Equivalent Circuit (b)

The circuit symbol and the basic equivalent circuit for a quartz resonator are shown in Figure 4.2.1-1. The symbol itself is made to represent the physical arrangement of the quartz sample mounted between the two electrodes. In the basic equivalent circuit, the series combination of C_1, L_1, and R_1 represents the quartz and C_0 represents the shunt capacitance of the electrodes and the metal housing. C_1 is connected with the stiffness of the quartz sample while L_1 is related to its mass. The resistor R_1 is due to oscillatory damping from the lattice itself and the mounting configuration [20: page 20-21, 23]. The RLC arm of the circuit is commonly referred to as the motional arm. The equivalent impedance is given in equation 4.2.1-1 [20: Appendix K]. Alternatively, the equivalent impedance can be calculated by a series combination of the motional impedances followed by a parallel impedance combination with the impedance of C_0.

$$Z = \frac{\left[\frac{-j}{2\pi f C_0}\right]\left[R_1 + j\left(2\pi f L_1 - \frac{1}{2\pi f C_1}\right)\right]}{\left[R_1 + j\left(2\pi f L_1 - \frac{1}{2\pi f C_1} - \frac{1}{2\pi f C_0}\right)\right]} \qquad (4.2.1\text{-}1)$$

The quality factor of the quartz resonator can be defined using several different equations. Equation 4.2.1-3 shows Q defined as the magnitude of the motional capacitive reactance divided by the motional resistance [30, 31]. Equation 4.2.1-4 shows Q defined as the magnitude of the motional inductive reactance divided by the motional resistance [20: page 29-30, 28]. Finally, equation 4.2.1-5 shows the generic Q defined in section 3.5.1 for a series RLC circuit. It will be shown in the next section that all three equations provide nearly identical results when evaluated using values measured from real quartz resonators.

$$Q_A = \left| \frac{X_{C_1}}{R_1} \right| = \frac{1}{2\pi f_s C_1 R_1} \tag{4.2.1-3}$$

$$Q_B = \left| \frac{X_{L_1}}{R_1} \right| = \frac{2\pi f_s L_1}{R_1} \tag{4.2.1-4}$$

$$Q_C = \frac{1}{R}\sqrt{\frac{L}{C}} \tag{4.2.1-5}$$

4.2.2 Measured Equivalent Circuit Parameters

During the quality assurance phase of manufacturing, quartz resonators are tested for conformance with any specified parameters. Measured data for the basic equivalent circuit parameters is shown in Table 4.2.2-1 below. This data was measured by the manufacturer to justify conformance to the required specifications. The data was measured at room temperature. The calculations of Q based on the measured data and equations 4.2.1-3, 4.2.1-4, and 4.2.1-5 shows that each of the three equations provides essentially the same results.

Table 4.2.2-1: MEASURED EQUIVALENT CIRCUIT PARAMETERS & CALCULATED Q FOR SEVERAL QUARTZ CRYSTAL RESONATORS

F_s (MHz)	Mode	C_0(pF)	$R_1(\Omega)$	C_1(fF)	L_1(mH)	Q_A	Q_B	Q_C
50.000000	3rd OT	4.1	15.0	1.80	5.6	117893	117286	117589
50.000000	3rd OT	4.0	14.9	1.86	5.4	114855	113856	114355
50.000000	3rd OT	4.1	16.7	1.59	6.4	119877	120396	120136
50.000000	3rd OT	4.0	15.2	1.91	5.3	109641	109542	109592
50.000000	3rd OT	3.9	14.5	1.90	5.3	115539	114831	115184
64.000000	3rd OT	4.4	35.8	1.55	4.0	44815	44930	44873
64.000000	3rd OT	4.4	21.5	1.53	4.0	75598	74814	75205
64.000000	3rd OT	4.5	28.9	1.68	3.7	51219	51483	51351
64.000000	3rd OT	4.5	18.7	1.61	3.8	82599	81715	82156
64.000000	3rd OT	4.4	19.0	1.55	4.0	84441	84658	84549
93.333333	5th OT	3.6	42.3	0.49	5.9	82271	81795	82033
93.333333	5th OT	3.6	61.4	0.47	6.2	59090	59216	59153
93.333333	5th OT	3.6	39.5	0.49	5.9	88103	87593	87848
93.333333	5th OT	3.6	39.2	0.50	5.8	87002	86768	86885
93.333333	5th OT	3.6	37.8	0.47	6.2	95983	96187	96085
200.000000	7th OT	4.8	42.5	0.41	1.5	45669	44352	45005
200.000000	7th OT	4.7	55.0	0.39	1.6	37099	36557	36827
200.000000	7th OT	4.7	49.6	0.38	1.7	42221	43070	42643
200.000000	7th OT	4.7	80.1	0.48	1.3	20697	20395	20546
200.000000	7th OT	4.9	44.5	0.41	1.5	43616	42359	42983

An analysis of the equivalent impedance of the basic equivalent circuit versus frequency using parameters from Table 4.2.2-1 clearly demonstrates the contribution of the C_0 arm and the motional arm respectively. The imaginary part of this equivalent impedance versus frequency is shown in Figure 4.2.2-1 using data from the first 64 MHz quartz resonator in Table 4.2.2-1. The C_0 contribution is the dominating exponential form that tends towards zero as the frequency increases, while the motional arm creates the deviation that can be seen at the resonant frequency of 64 MHz.

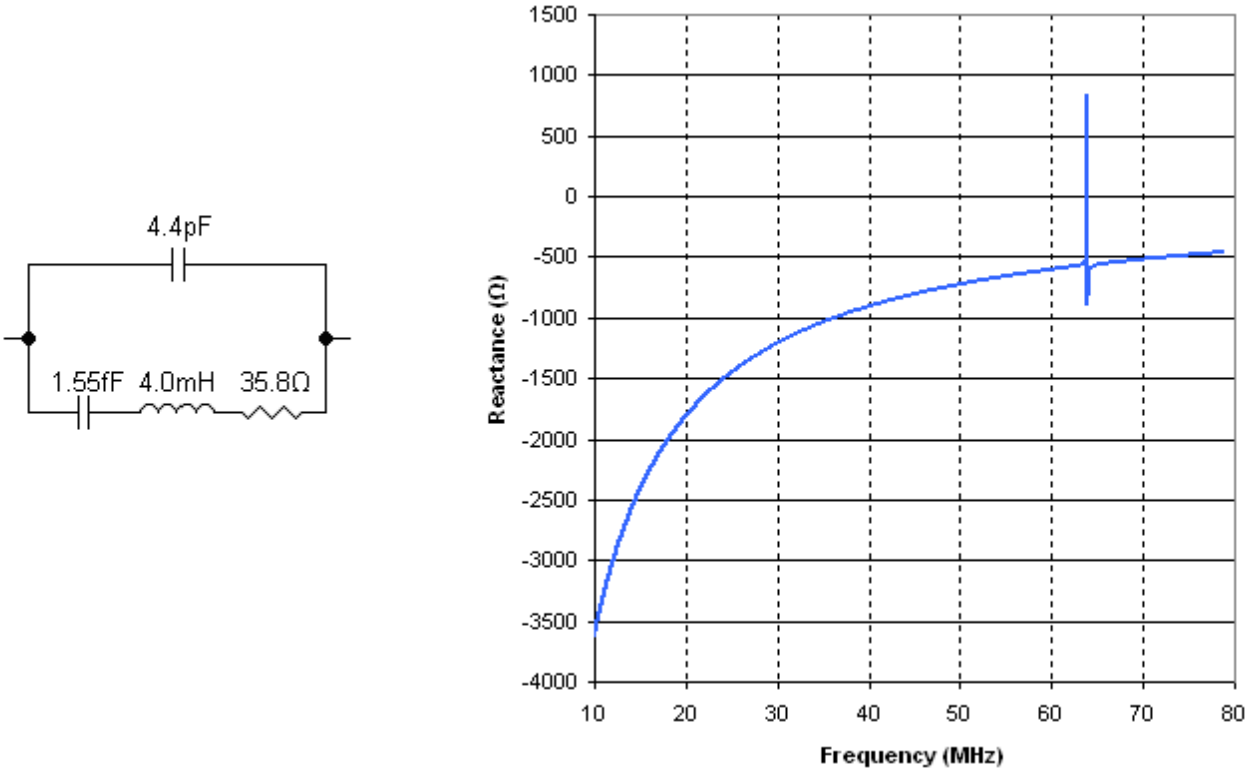

Figure 4.2.2-1: 64 MHz Equivalent Circuit & Reactance Curve for the First 64 MHz Quartz Resonator in Table 4.2.2-1

The series resonant frequency (f_s) of the quartz resonator is defined as the frequency at which the reactance of the equivalent circuit is zero and is given by equation 4.2.2-1 [20: page 21, 31]. From Figure 4.2.2-1, it is evident that the reactance is zero only at the deviation caused by the motional arm. A close-up of the frequency range around f_s is shown in Figure 4.2.2-2. It may seem strange that the resonance is not at 64 MHz exactly, but that is merely due to the equivalent circuit parameters having been rounded to so few significant figures. The actual resonator will have an f_s within several parts per million (ppm) of 64 MHz.

$$f_s = \frac{1}{2p}\frac{1}{\sqrt{L_1 C_1}} \qquad (4.2.2\text{-}1)$$

At f_s, the reactance is zero and the resonator is purely resistive. Furthermore, the magnitude of the impedance is at a minimum allowing maximum current flow. At frequencies slightly above f_s, the resonator appears inductive. When the reactance of the motional inductance equals the reactance of C_0, the equivalent reactance again crosses zero. This is generally called the anti-resonance frequency (f_a) and is given by equation 4.2.2-2 [20: page23, 31]. At f_a, the magnitude of the impedance is maximized and current flow is minimized – making this point unstable for use in an oscillator [28]. According to equations 4.2.2-1 and 4.2.2-2, f_s and f_a are 63918163 Hz and 63929421 Hz – which agree well with Figure 4.2.2-2.

$$f_a = f_s\left[1+\frac{C_1}{2C_0}\right] \qquad (4.2.2\text{-}2)$$

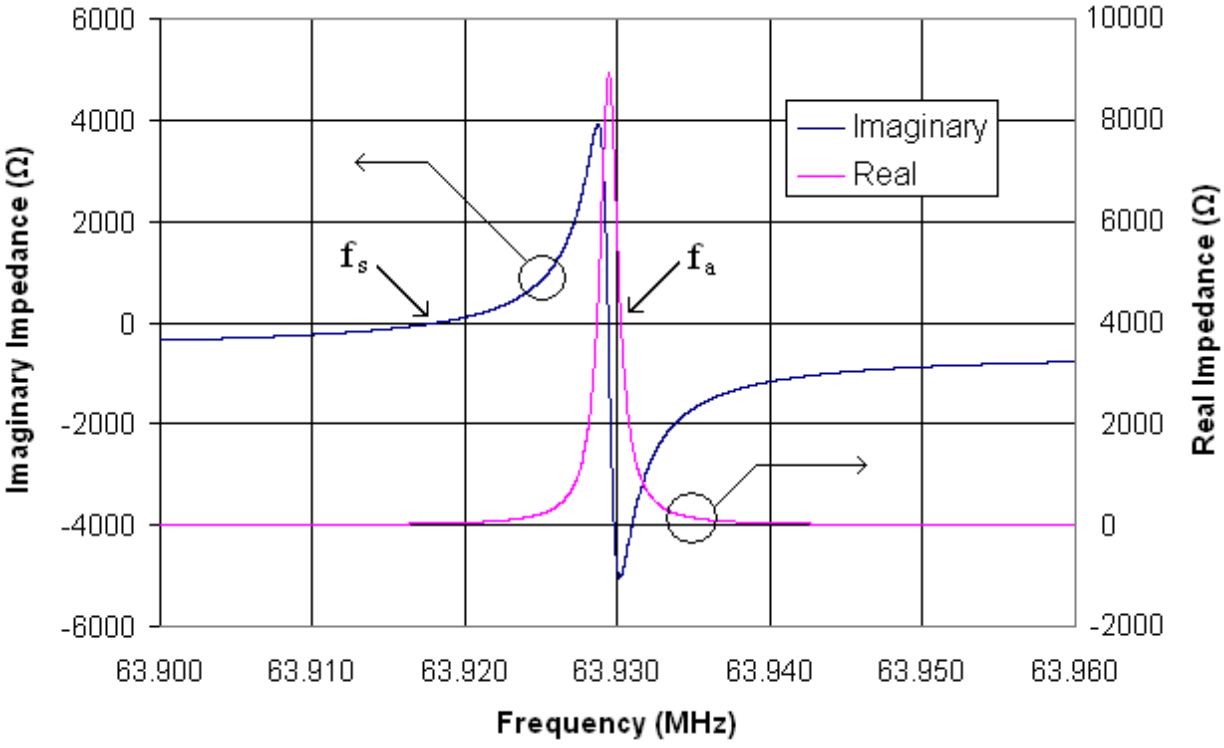

Figure 4.2.2-2: Close-Up of Motional Arm Resonance

Between f_s and f_a is the area of parallel resonance where the resonator reactance appears inductive. An external load capacitance added in series with the quartz resonator will result in a negative shift of the reactance versus frequency curve. This will produce a positive shift Δf in the frequency at which the resonator is series resonant. This new loaded series resonant frequency can be called f_L and is the sum of f_s and Δf. If the external load capacitance C_L is known, the positive shift Δf can be calculated using equation 4.2.2-3 [20: page 22, 31]. If the external load capacitance is electronically variable, such as the varactor diode discussed in section 3.6, the resonant frequency can be dynamically adjusted by an electronic control circuit.

$$\Delta f = f_s \left[\frac{C_1}{2(C_0 + C_L)} \right] \qquad (4.2.2\text{-}3)$$

Strictly speaking, the load capacitance C_L is a combination of any discrete capacitance intentionally placed in series with the resonator (such as a varactor) and any additional capacitance presented by the remainder of the oscillator circuitry. For this reason, it is important that some approximation of the cumulative load capacitance C_L be known when the quartz resonator is being specified. This information will allow the manufacturer of the quartz resonator to create a resonator that, when placed into the circuit with the specified load capacitance C_L, will produce the desired nominal loaded series resonant frequency f_L. If C_L is not accounted for when specifying the resonator, an unexpected frequency offset Δf may result when the resonator is placed in the oscillator circuit. This may render the resonator unusable or force the oscillator circuit to be redesigned to achieve the desired loaded series resonant frequency f_L.

Since f_L must be between f_s and f_a, the area of parallel resonance, a quartz resonator whose f_s and f_a are farther apart can be made resonant on a greater range of frequencies. This bandwidth is inversely proportional with the capacitance ratio r of the quartz resonator where r is defined in equation 4.2.2-4 [28, 31]. The capacitance ratio is a measure of the interconversion between electrical and mechanical energy stored in the crystal lattice [28].

$$r = \frac{C_0}{C_1} \tag{4.2.2-4}$$

Furthermore, r increases with the square of the OT number [28]. This is shown in Table 4.2.2-2 where r and the percent bandwidth (%BW) have been calculated for the data in Table 4.2.2-1 and averaged by OT. The %BW is calculated using equation 4.2.2-5 where f_{NOM} is the nominal frequency (listed as F_s) in the first column of Table 4.2.2-1. The %BW is used because comparing absolute bandwidths at widely separated frequencies can be misleading. Table 4.2.2-2 confirms that r increases with OT and %BW decreases with r.

$$\%BW = \left[\frac{(f_a - f_s)}{f_{NOM}}\right] \times 100\% \tag{4.2.2-5}$$

Table 4.2.2-2: CAPACITANCE RATIO & % BANDWIDTH BY OVERTONE

Mode	r	%BW	% BW Normalized
3rd OT	2518	0.020229	1
5th OT	7443	0.006729	0.333
7th OT	11574	0.004381	0.217

4.2.3 Advanced Equivalent Circuit

Having introduced the basic equivalent circuit and seen the reactance versus frequency for a single motional arm and a C_0 arm (Figure 4.2.2-1), it is possible to introduce additional motional arms to the basic equivalent circuit to increase its accuracy. Just like the reactive components L and C in chapter 3 possessed undesired parasitic resistance, the quartz resonator possesses additional parasitic resonant behavior not seen in the analysis of the basic equivalent circuit. Full understanding of the complete frequency response of the resonator will enable a designer to create a circuit that will produce the desired results regardless of the parasitic resonances. Note that defining the alternative resonances as parasitic is subjective and based on the definition of a particular resonance as desired.

Since Table 4.2.2-1 states that 64 MHz is the 3rd OT of the quartz resonator, it is logical to add a motional arm representing the fundamental mode of the thickness shear resonance. A motional arm representing the 5th OT thickness shear mode will also be added. The resulting expanded equivalent circuit and equivalent reactance versus frequency curve is shown in Figure 4.2.3-1. The new motional arm element values are approximate and are designed to curve-fit the equivalent circuit frequency response to a measured plot of the broadband frequency response made using a scalar network analyzer. The exponential trend from the C_0 term is still visible in the blue reactance versus frequency curve – which is referred to the axis on the left. Additionally, there are three motional arm disturbances – 21.333 MHz, 64.000 MHz, and 106.667 MHz representing the fundamental, 3rd OT, and 5th OT modes respectively. This figure shows more clearly than Figure 4.2.2-1, why a second resonant circuit is necessary in an oscillator that requires a quartz resonator to operate on one of its OTs. The second

resonant circuit operates as a bandpass filter that attenuates parasitic modes of oscillation that might otherwise dominate the oscillator (in this example, the fundamental and 5th OT). The bandpass response of the second resonant circuit is plotted in red and is referred to the axis on the right. Its passband (frequency range where attenuation is near 0 dB) can be seen to coincide with the 64 MHz 3rd OT. It is this method of OT selection using a second resonant circuit that allows the traditional AT cut quartz resonator to be used in oscillators up to the 7th OT or even higher.

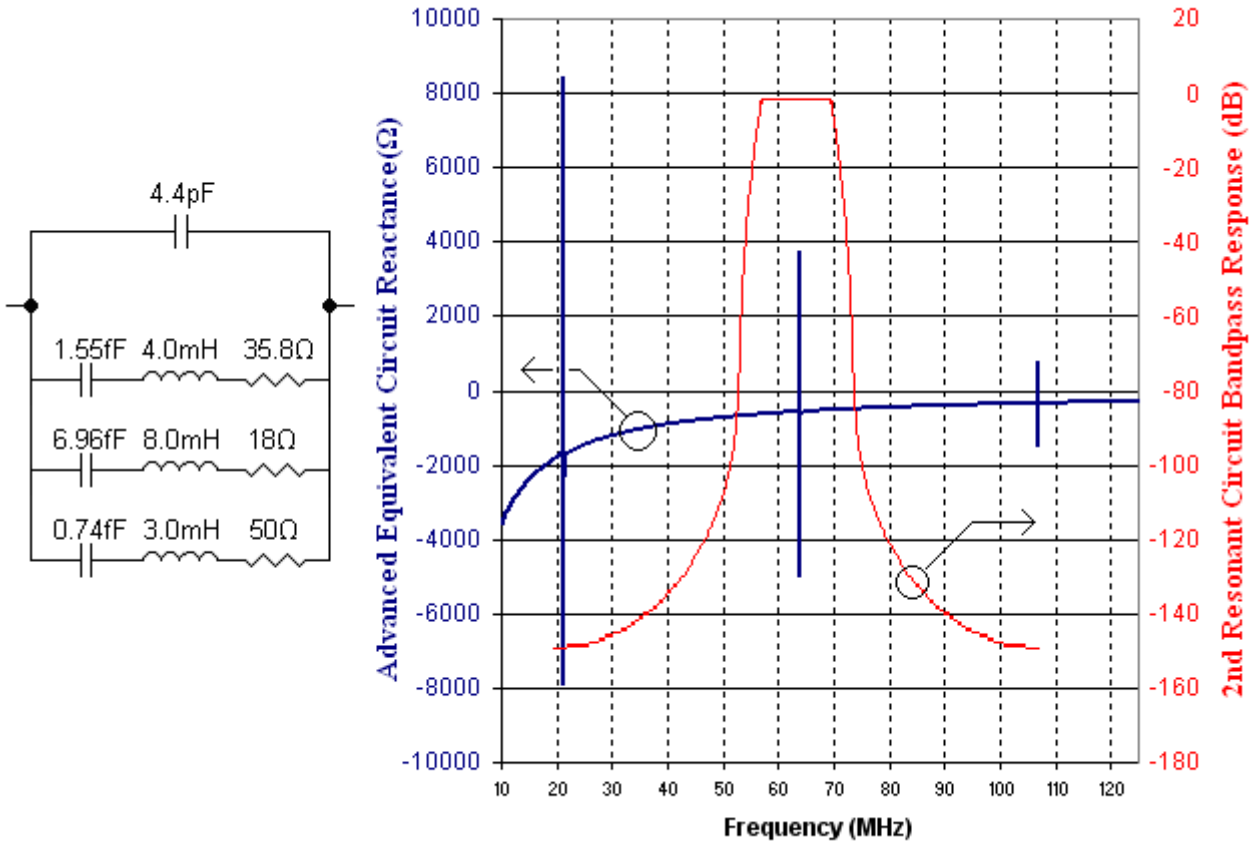

Figure 4.2.3-1: 64 MHz Advanced Equivalent Circuit with Reactance Curve (blue) and 2nd Resonant Circuit Bandpass Response (red) Versus Frequency

If the oscillator is to function on the fundamental mode, a second resonant circuit is rarely required because, as seen in Figure 4.2.3-1, the fundamental mode has the lowest motional resistance and will generally dominate unless attenuated intentionally. Overtone mode oscillator circuits, like the one that will be introduced in the next chapter, require intentionally introduced attenuation of strong parasitic modes. Whether the oscillator is to function on the fundamental or an OT, the equivalent circuit does not need to show the parasitic motional arms to provide good analytical or simulated results. In the case of an OT oscillator equipped with a well designed second resonant circuit, the attenuation of the parasitics is generally so effective that their contribution becomes insignificant. Furthermore, when the parasitic motional arms are removed from the advanced equivalent circuit shown in Figure 4.2.3-1, it reduces back to the basic equivalent circuit discussed in the previous two sections. It is for this reason that most literature only discusses the basic equivalent circuit.

4.2.4 Practical Limitations of the Traditional Quartz Resonator

While selection by a secondary resonator allows oscillation on desired OTs, realistic limits exist on how high of an OT may be practically used. It is clear from Figure 4.2.3-1 that the resonances become weaker as the OT increases. The amplitude of the reactance disturbance from a motional arm is inversely proportional to the motional resistance in the respective arm. Furthermore, the shear mode motional resistance increases with OT order. This is a direct result of the piezoelectric properties of the lattice. Recall that the lattice must flex a number of times equal to the OT number as shown previously in Figure 4.1-1. High order flexure within the lattice is resisted more and more by the strength of the lattice itself.

Another limiting phenomenon exists in the form of the spurious resonances. Spurious modes of vibration are all the parasitic resonances that are not the fundamental or OT thickness shear modes. In the AT cut resonator, the spurious modes occur above each main response within several hundred kHz [20: page 31, 28]. If a spurious response exists very close to the desired response and has a sufficiently low spurious arm motional resistance, the circuit may oscillate on the spurious rather than on the main mode – this is known as mode hopping [28]. It is the presence of these parasitic spurious modes and their interaction that creates the largest problem with operating the resonator at high OT modes. Since spurious modes exist well within the passband of the second resonant circuit, alternative methods must be employed to mitigate their effect. Since control of the design of the quartz sample, the electrode pattern, and amount of metallization are the most effective methods of mitigating the effect of spurious modes in the resonator, it is important to specify to the resonator manufacturer that spurious modes within a certain frequency range of the desired response possess motional resistance greater than that of the desired response by some factor [28]. A spurious motional resistance of three to five times higher than that of the desired response across the full range of operating temperature is typically sufficient to prevent oscillations on a spurious mode [28, 20: pages 31, & 128]. As OT order increases, the operative motional resistance increases, making it progressively more difficult to maintain a high spurious to primary resistance ratio [28]. This drives up the cost of the resonator and opens the door for stability issues in the oscillator due to insufficiently mitigated spurious modes.

Adding motional arms to the equivalent circuit for the spurious modes is identical to the example in the previous section of adding the fundamental and 5^{th} OT motional

arms. However, when the reactance is plotted versus frequency, the spurious modes appear within several MHz of the desired response. With the addition of OT and spurious motional arms, the equivalent circuit is fully accurate under normal operating conditions.

In conclusion, due to the lattice damping of high OTs and the difficulty of increasing spurious modes, it is desirable to operate on as low an OT as possible. Furthermore, from section 4.2.2 lower OTs provide greater area of parallel resonance, which means larger tunable bandwidth. However, operating on a lower OT of thickness shear mode dictates that the sample is made thinner. Since, there is a finite limit to how thin and fragile the sample can be made using traditional cutting and grinding techniques (see Figure 4.2.4-1), it is desirable to operate on higher OTs of a thicker and more robust sample. These limiting factors impose the practical upper boundary to the frequency range of the AT cut quartz resonator as it has been traditionally manufactured.

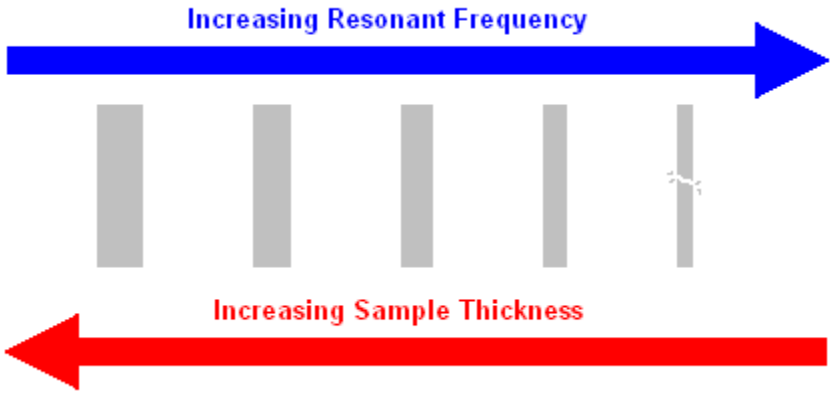

Figure 4.2.4-1: Thickness vs. Resonant Frequency for Traditional Resonator

4.3 Inverted-Mesa Etched Quartz Resonator

The inverted-mesa etched quartz resonator enables oscillation on lower OTs by allowing thinner quartz samples than are possible using traditional fabrication techniques [32, 33]. Initially, the sample is prepared using traditional methods. However, additional processing is added where the cut and ground wafer is then partially exposed to an etchant such as sodium hydroxide that dissolves exposed quartz at a known rate. Since the etch rate is determined by selection of etchant and temperature control, the depth can be carefully managed by controlling the duration of the reaction. A mask of some kind is placed such that the perimeter of the wafer is protected from the etchant while the center of the wafer is exposed. The etching can be on one or both sides of the center of the wafer. Since the perimeter is not etched, the result is a very thin center surrounded by a thick outer rim (see Figure 4.3-1). The rim provides strength and rigidity to the sample, while the thin center provides a much thinner resonant section than would be feasible were the entire wafer required to be of the same thickness – as in traditional fabrication. This type of quartz resonator has been fabricated to thicknesses with fundamental thickness shear modes as high as 620 MHz and 2000 MHz [34, 35] respectively.

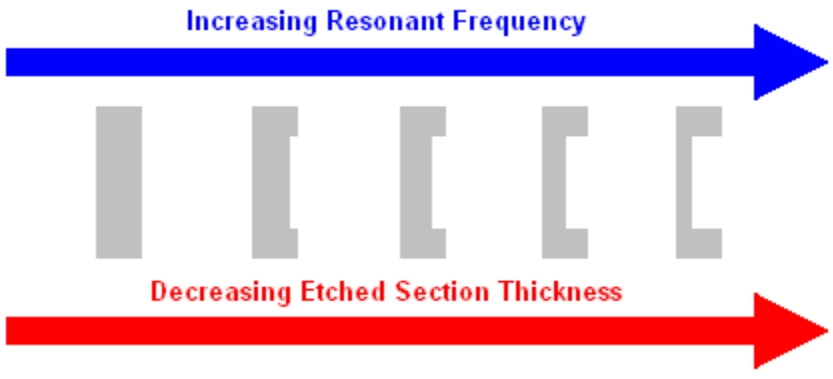

Figure 4.3-1: Thickness vs. Resonant Frequency for Etched Resonator

It is, therefore, the ultimate motivation of the current work to design an oscillator circuit that operates using an inverted-mesa etched quartz resonator as its frequency selective feedback network. More specifically, an oscillator that has operated successfully with a traditionally manufactured quartz resonator will be enhanced to accommodate the new resonator type. Full performance will be verified and relevant comparative data will be measured. Employing the advantages of the inverted-mesa etched resonator will enable the extension of the low noise quartz resonator oscillator beyond its previous frequency limitations. This new oscillator will, therefore, meet and exceed the current demand for lower phase-noise radio frequency synthesizers and ultra-low jitter system clocks and can enable performance advances in a wide range of applications.

CHAPTER 5
THE TWO-TRANSISTOR BUTLER OSCILLATOR – INTRODUCTION, SIMULATION, FABRACATION, AND MEASURED RESULTS

5.1 Introduction and Circuit Discussion

In this section, a functioning oscillator will be introduced, and various previously mentioned performance parameters will be measured from the oscillator and compared for two different types of resonant circuit. Before introducing the actual oscillator circuit schematic, however, it should again be noted that almost infinitely many circuit configurations exist for electronic oscillators. The circuit used here is popular for use with OT quartz crystal resonators and is commonly known as the Two-Transistor Butler Oscillator [36: chapter 11, 37: pages 58-65 & 144-156]. It is a variation of the Grounded-Base Oscillator [20: pages 89-100]. It is more easily understood if it is built up from the most basic model presented earlier in section 3.2. In Figure 5.1-1 below, the most basic model is expanded to include a second resonant circuit and amplifier. As previously mentioned, when using an OT quartz resonator as the frequency selection device for an electronic oscillator, a second resonant circuit must be present to suppress oscillation on the fundamental thickness shear mode of the quartz resonator and any OTs lower than the one desired. This second resonant circuit (labeled “LC Resonant Circuit” in Figure 5.1-1), performs this OT selection function. While two amplifiers are not strictly necessary, they help isolate the two resonant circuits and also greatly improve the gain and stability of the oscillator. Another important feature of Figure 5.1-1 is that the OT quartz resonator has been labeled as tunable. Compensating for temperature induced frequency drift and

resonator aging induced frequency drift are the primary reasons for requiring tunability in the crystal oscillator (XO).

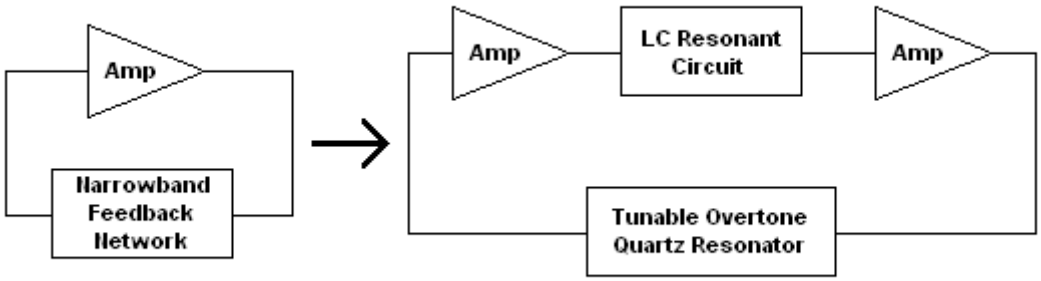

Figure 5.1-1: Expansion of Most Basic Oscillator Model

The oscillator schematic in Figure 5.1-2 reveals that the EFC is accomplished by implementing a varactor diode (labeled U_1) in series with the quartz resonator – as discussed in section 4.2.2. An RF blocking resistor R_{b1} of 30 $k\Omega$ and a DC blocking capacitor C_{b1} help ensure that the DC voltage supply Vtune can provide the tuning voltage to the varactor but not load the resonator or bias the emitter of transistor Q1 respectively. Furthermore, another 30 $k\Omega$ resistor R_{b2} to ground on the U_1 varactor opposite Vtune is required for proper operation and does not load down the oscillator. The tunable OT quartz resonator is connected to the two transistor stages by AC coupling capacitors C_{b1} and C_{b2} (which can alternatively be referred to as DC blocking capacitors). Excluding the Vtune source as it is merely a placeholder for an EFC circuit, the circuit is known as a voltage controlled crystal oscillator (VCXO).

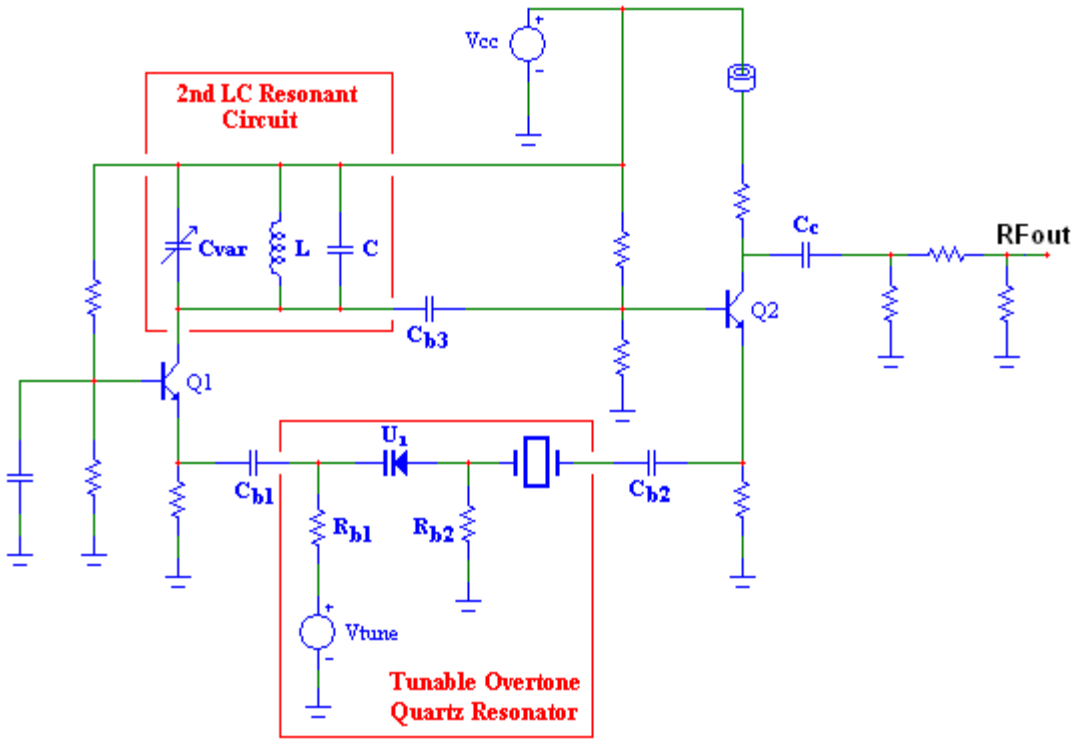

Figure 5.1-2: Two-Transistor Butler Voltage Controlled Crystal Oscillator

The common-base configuration of transistor Q1 in conjunction with the second LC resonant circuit as its collector bias is a narrowband voltage amplifier and current buffer [19: pages 435-438]. This narrowband stage is a very effective OT selection circuit and presents low resistance to the tunable quartz resonator [19: pages 437-438]. The second LC resonant circuit is constructed using a fixed inductor L and capacitor C in parallel with a manually adjustable capacitor Cvar. The values should be selected such that the parallel resonant frequency of the three elements corresponds with the desired OT. The coarse tuning of OT selection is accomplished by changing either the fixed inductor L or capacitor C. The variable capacitor Cvar is most useful for centering the EFC range about the desired nominal frequency. Similar to the way the variable series capacitance of the varactor diode pulls the resonant frequency of the quartz resonator, the

second LC resonant circuit also interacts somewhat with the quartz resonator to provide another point of frequency control. Using this variable capacitor Cvar for fine centering becomes a convenient way to compensate for small variations from one transistor to the next or slight resonant frequency variations from one tunable quartz resonator to the next.

The output of the narrowband common-base stage is AC coupled via C_{b3} to the second stage. The second stage transistor is Q2 and is in either an emitter-follower or a common-emitter configuration depending on whether the output is considered to be in the feedback direction towards the quartz resonator or in the forward direction towards the oscillator load at RFout [19: pages 399-435]. This is very practical as the emitter-follower seen by the resonator provides current gain and presents a low resistance, while the common-emitter amplifier seen by the oscillator load at RFout provides both voltage and current gain and presents a moderate to high output resistance. Also, since the input is into the base of Q2, the input resistance is moderate to high [19: page 440].

A series capacitor C_c is connected to the collector of transistor Q2 to AC couple energy out to the oscillator load. A water tower is a useful analogy for understanding the importance of the coupling capacitor C_c. If more water is drawn from a water tower than is being pumped into it, the tower will be emptied and cease to meet demand. Similarly, the value of the series coupling capacitor C_c must be carefully selected so that the impedance of the capacitor at the oscillator frequency is low enough to couple out enough energy to be useful, but not so low that the oscillations become overdamped and die out. The energy is then passed through a 3dB “pi” configuration resistor attenuator that also helps match the output connection to 50 Ω for transmission through 50 Ω SMA cables.

5.2 Transient Simulation

The oscillator circuit shown in Figure 5.1-2 was assembled in the evaluation version of Micro-Cap 9.0.1.0 by Spectrum Software. A transient simulation was performed to confirm that the circuit would be capable of developing and maintaining steady state oscillations. The resulting waveform showing the node voltage at the collector of Q2 is shown in Figure 5.2-1 and does indeed confirm that the circuit builds up to steady state oscillations. Figure 5.2-2 shows a close-up of the waveform shown in Figure 5.2-1.

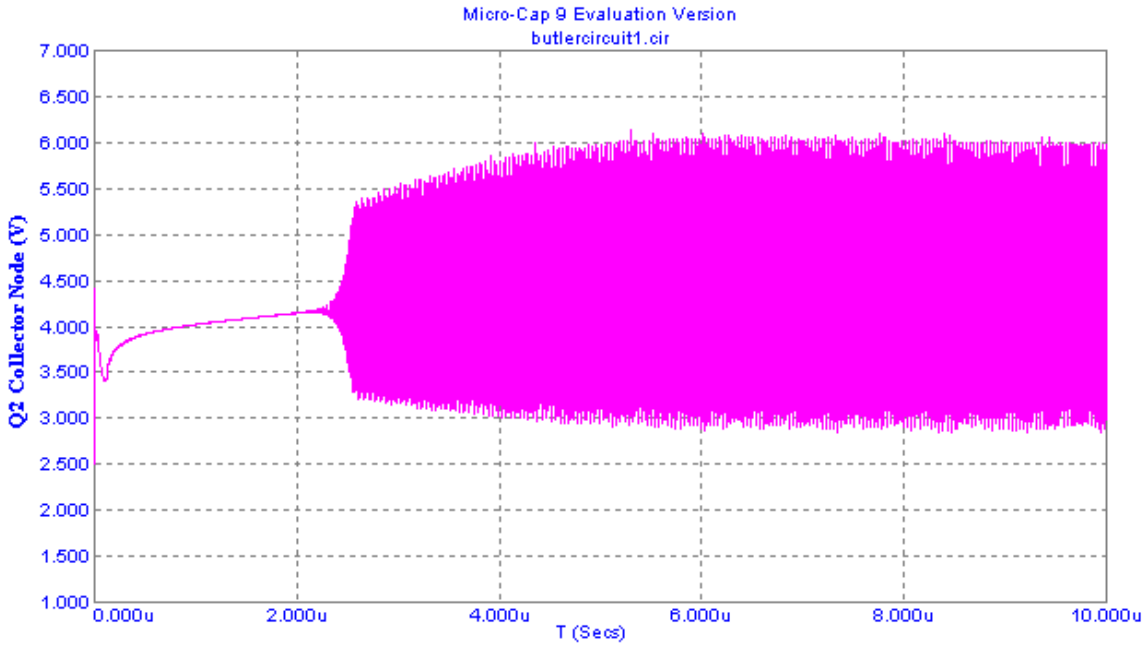

Figure 5.2-1: Startup of Steady State Oscillations in Circuit Simulation

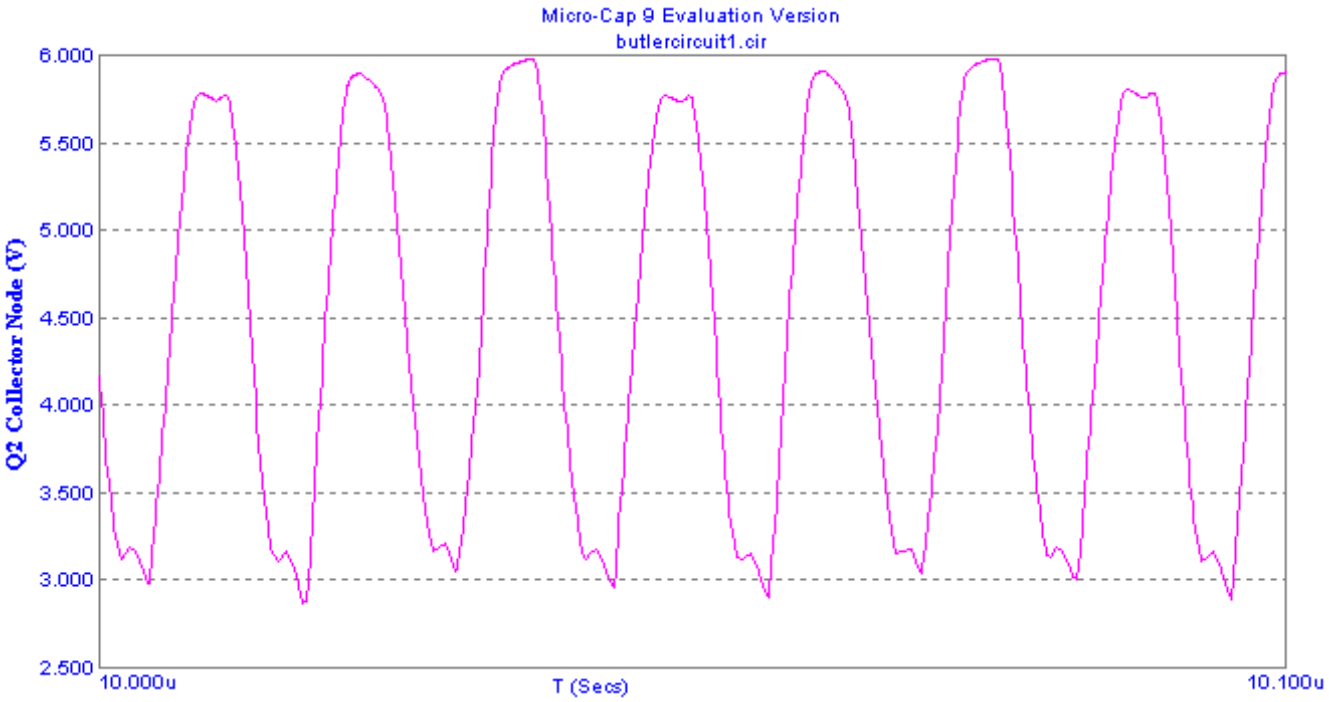

Figure 5.2-2: Close-Up of Oscillations on Q2 Collector Node

5.3 Measured Results from 64MHz VCXO

A photograph of the constructed circuit is shown in Figure 5.3-1. The layout of the circuit is very similar to the schematic shown in Figure 5.1-2 with added red outlining and labels for Q1, Q2, and the 64 MHz quartz resonator. Plated through holes connect the solid ground plane on the backside with lands on the top side of the printed circuit board (PCB) so that elements that are in shunt to ground can be easily soldered – such as C_1 which is a capacitor with one end connected to the Vtune line (or trace) and the other end connected to a land that is connected to ground by the plated through hole at A (and the four other plated thru holes that can be seen on the same land). The manually adjustable capacitor labeled Cvar can be seen to be adjustable with a precision flat-head screwdriver. The two transistors are in the three leaded black plastic packages to the farthest left and right and are marked by “Q1” and “Q2” annotations. The varactor diode

is in a similar package as the transistors but can be distinguished by its direct connection to the quartz resonator lead closest to Q1 as shown in the schematic. As for the smaller components, the ones with a black section between the two metal terminations, such as R, are resistors and the ones with a tan section between the two metal terminations, such as C, are capacitors. To provide a scale, a tantalum power supply decoupling shunt capacitor near VCC measures approximately 0.140 in. long (X) by 0.110 in. wide (Y).

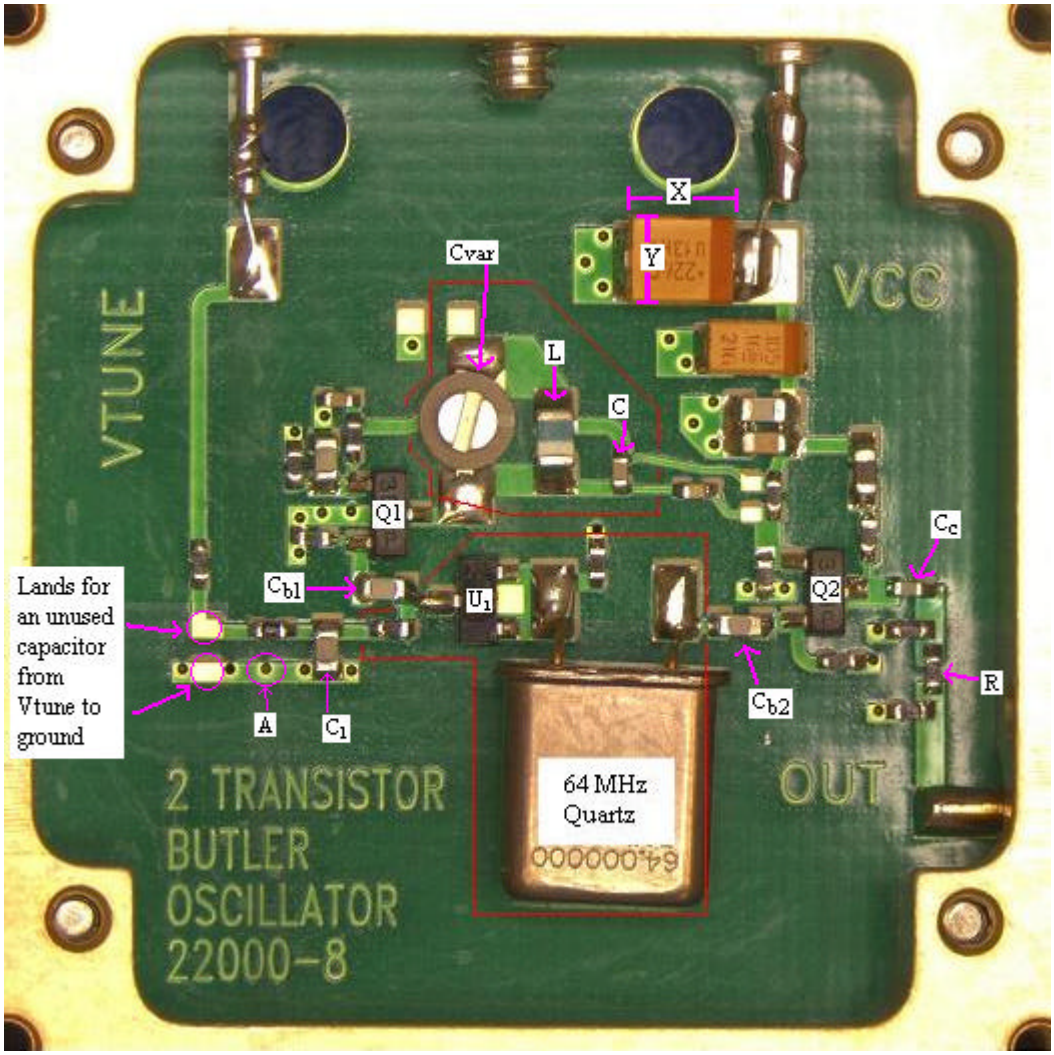

Figure 5.3-1: Photograph of the Fabricated VCXO Circuit with Labels

Once constructed, the oscillator's VCC shown in Figure 5.3-1 was connected to a +5 volt DC power supply. The steady state oscillations on the collector of Q2 are shown in Figure 5.3-2 using a Tektronics® TDS3032B oscilloscope. The oscilloscope is specialized at capturing the time domain voltage waveform and accurately displays the voltage magnitude and the wave shape of the signal.

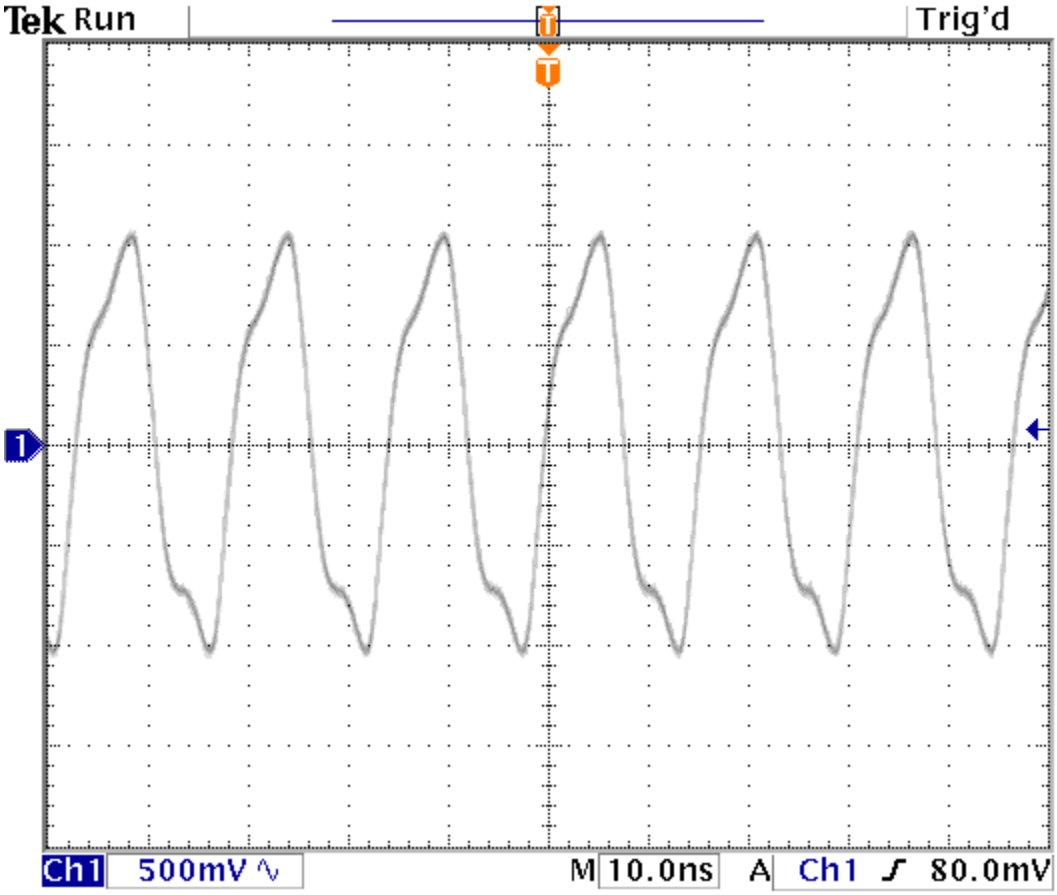

Figure 5.3-2: Measured Voltage Oscillation at Q2 Collector Node

Just as the oscilloscope is specialized for capturing the voltage waveform in the time domain, the spectrum analyzer is an instrument that is specialized in the display of signal power in the frequency domain. The circuit's Vtune was connected to another voltage supply and the output was connected to the spectrum analyzer. The tuning voltage supply was adjusted until the Hewlett Packard 8563E spectrum analyzer read approximately 64 MHz. Figure 5.3-3 is a photograph of the spectrum analyzer showing the signal on the port labeled "OUT" in Figure 5.1-3. Note the similarities between the spectrum analyzer measurement in Figure 5.3-3 and Figure 1-1.

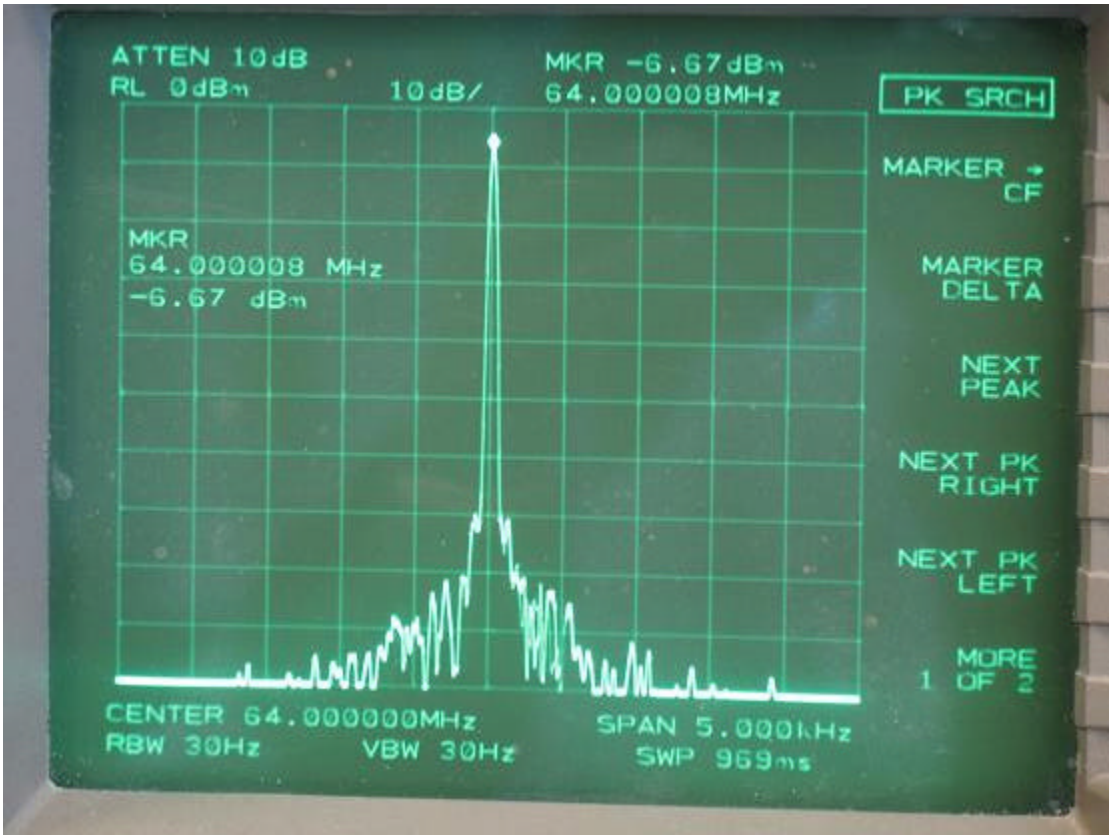

Figure 5.3-3: Spectrum Analyzer Display for Centered 64 MHz VCXO

CHAPTER 6
TUNING THE OSCILLATOR FROM 64 MHZ TO 200 MHZ

6.1 Purpose and Method

The VCXO has been shown to function using a 64 MHz quartz resonator, but it is necessary to tune it to higher frequencies to take advantage of the benefits of the inverted-mesa etched quartz resonator. In this chapter, the process of tuning the oscillator from resonance at 64 MHz to 200 MHz will be described. The first step in accomplishing this is to substitute the quartz resonator with a series RLC circuit with resonance near 200 MHz. With this circuit in place, the second LC resonant circuit in the common-base narrowband amplifier will also be tuned to approximately 200 MHz. At this point, the oscillator should output approximately 200 MHz. If it does not, then it is likely that the transistors in use are incapable of supporting such high frequencies, and new transistors would need to be substituted. Once operating, the EFC bandwidth and oscillator phase noise will be measured.

Once the oscillator is functional with the series RLC circuit at 200 MHz, a quartz resonator designed for this frequency will be reinstalled in place of the RLC circuit. The circuit will then be a VCXO at 200 MHz and the EFC bandwidth and oscillator phase noise will again be measured. In addition to retuning the oscillator, this method will also provide EFC bandwidth and phase noise data that will clearly illustrate the advantages and disadvantages of the quartz resonator based oscillator versus a series discrete RLC circuit. The EFC bandwidth and phase noise performance will be compared to illustrate some of the claims made in prior chapters regarding the relationships between Q, EFC bandwidth, and phase noise performance.

6.2 Retuning & Performance with 200 MHz Series RLC Resonator

The 64 MHz quartz resonator is removed from the circuit used in the previous chapter and shown in Figure 5.3-1. A series RLC circuit comprised of R = 10 Ω, L = 27 nH, and C = 22 pF produces a resonant frequency of approximately 206 MHz and uses readily available discrete component values. Though the resistor does not influence the resonant frequency, it is an important addition as a representation of the motional resistance that the quartz resonator will possess. Next, the second resonant circuit in the narrowband amplifier is also retuned to approximately 200 MHz.

At this point, the retuned oscillator was connected to an Agilent® E5052A Signal Source Analyzer. This is an instrument very specialized in characterizing the various parameters of VCOs and VCXOs. The E5052A has tune voltage and DC power outputs that connect to the Vtune and Vcc oscillator inputs respectively. It also has an RF input that connects to the output of the oscillator under test. The tune voltage output was configured to sweep in even steps from 0 V to +5 V and the DC power output was set to a fixed +5 V. The circuit produced stable oscillations indicating that the transistors are still capable of operation at the new frequency. Next, the E5052A was configured to record measurements of the oscillator output frequency in MHz, EFC tuning sensitivity in MHz/V, oscillator output power in dBm, and Vcc supply current in mA versus the sweeping EFC tuning voltage Vtune. Only the E5052A and the oscillator under test are required for the measurement sweep. Figure 6.2-1 shows the E5052A graphs of these four parameters as functions of the sweeping EFC tuning voltage Vtune. As seen in the plots and the selected data shown in Table 6.2-1, the oscillator is resonant and tunable about the desired nominal frequency of 200 MHz.

Additionally, the VCO has an EFC bandwidth of approximately 13.5 MHz or 67500 parts per million (ppm)[1], output power variation of less than 2 dB over the EFC band, and less than a 1 mA of variation in supply current. Ideally, the tuning sensitivity would be consistent across the EFC band (meaning the VCO would have a perfectly linear relationship between EFC voltage and output frequency), but the trend seen is sufficiently linear to be used over smaller subsets of the overall range.

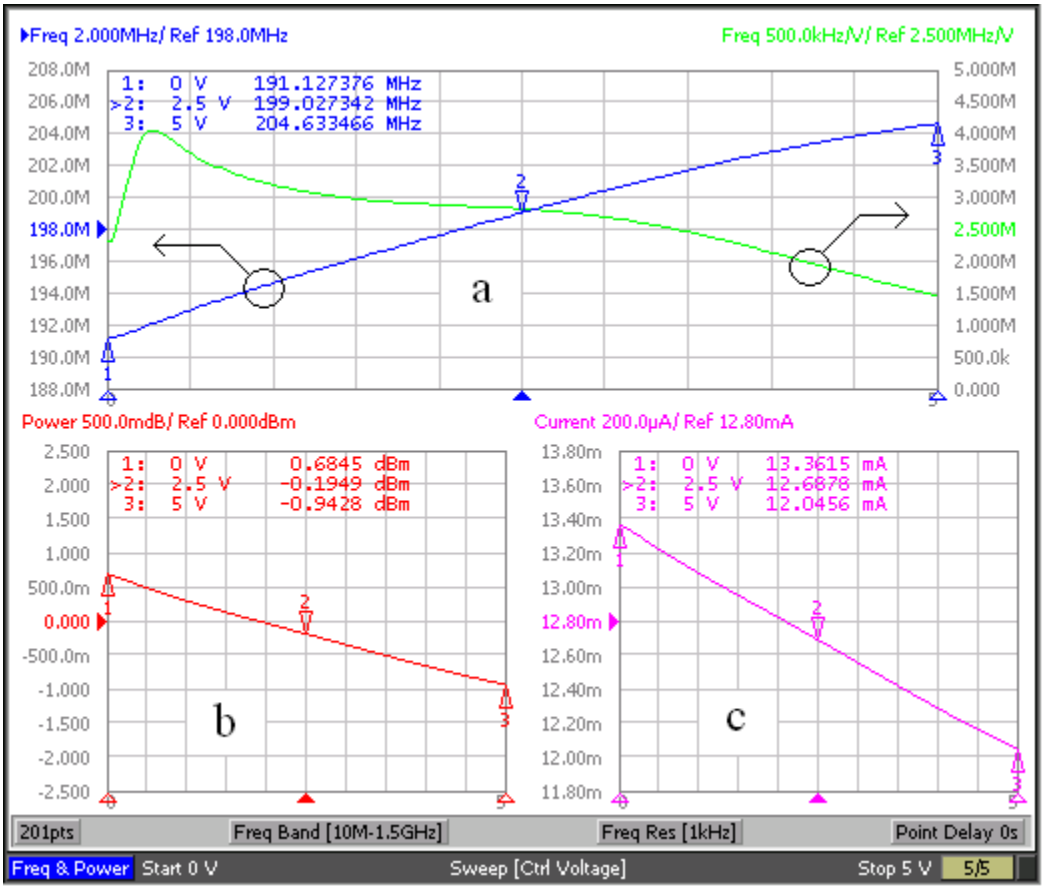

Figure 6.2-1: Swept EFC Measurements with 200 MHz Discrete Series RLC Resonator. (a: blue) Oscillator Output Frequency. (a: green) Oscillator EFC Tuning Sensitivity. (b) Oscillator Output Power. (c) Oscillator Supply Current

[1] At 200 MHz, $1\,\text{ppm} = \frac{200\,[\text{MHz}]}{1000000} = 200\,[\text{Hz}]$. So, $13.5\,[\text{MHz}]\frac{1\,[\text{ppm}]}{200\,[\text{Hz}]} = 67500\,[\text{ppm}]$.

Table 6.2-1: SELECTED MEASURED DATA WITH RLC RESONATOR

DC Tuning Voltage (V)	RFout (MHz)	Tuning Sensitivity (kHz/V)	Output Power (dBm)	Supply Current (mA)
0.00	191.127376	2313.272	0.685	13.361
0.50	192.902654	3689.346	0.483	13.223
1.00	194.604434	3194.922	0.293	13.081
1.50	196.139515	2976.695	0.124	12.950
2.00	197.601398	2886.231	-0.037	12.820
2.50	199.027342	2815.602	-0.195	12.688
3.00	200.408093	2692.942	-0.355	12.552
3.50	201.699623	2458.660	-0.513	12.418
4.00	202.849534	2132.957	-0.667	12.287
4.50	203.827102	1780.360	-0.812	12.162
5.00	204.633466	1467.004	-0.943	12.046

Next, the phase noise measurement feature of the E5052A was used with the EFC tuning voltage set to a fixed 2.5 V rather than a sweep. The measurement graph is shown in Figure 6.2-2. Though phase noise is truly a symmetrical double sideband phenomenon as shown in Figure 1-1, it is usually represented in plots showing only a single sideband (SSB). The spectral density of the phase noise is represented in decibels relative to the carrier or center frequency in a per Hertz of bandwidth (dBc/Hz) [18: page 594]. Plots like Figure 6.2-2 are common and the horizontal axis represents the offset from the center frequency of the oscillator (carrier frequency) while the vertical axis is the relative power of the phase noise to the center frequency or carrier. Finally, the contribution to the time jitter from the phase noise in Figure 6.2-2 was calculated by the E5052A to be 1330 ps – as seen in Figure 6.2-3. The E5052A automatically calculates the time jitter from the phase noise using methods similar to those in references [17, 8, and 12].

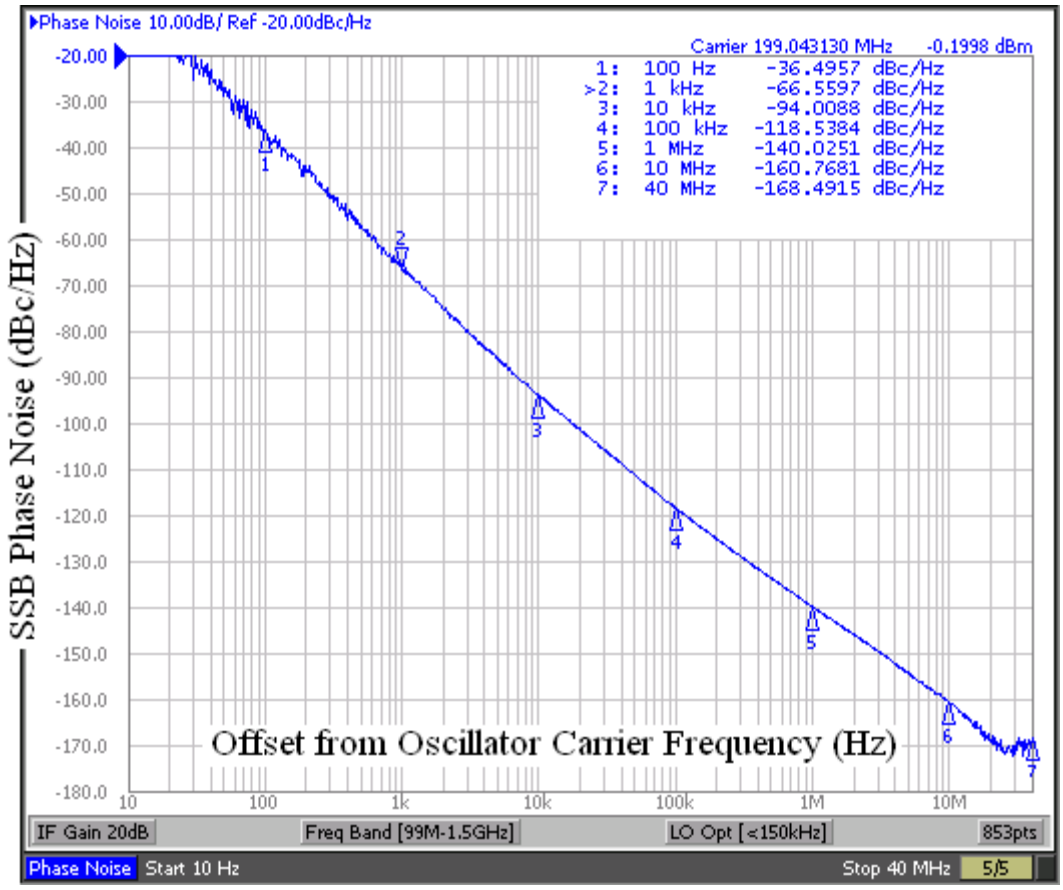

Figure 6.2-2: E5052A Phase Noise Measurement with 200 MHz Series RLC Resonator

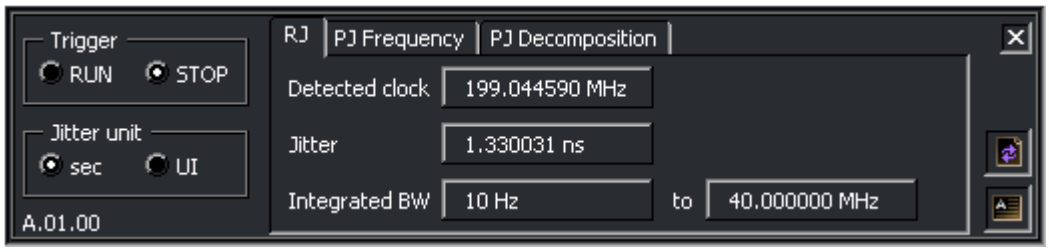

Figure 6.2-3: E5052A Time Jitter Integration with Series RLC Resonator

6.3 Performance with Traditional 200 MHz Quartz Resonator

With the oscillator capable of functioning at 200 MHz using a series RLC resonator, a 200 MHz quartz resonator will now be substituted back into the circuit and it will appear nearly identical to Figure 5.3-1 once again. A traditionally manufactured quartz resonator will be substituted. Initially, a 7th OT resonator (approximately 28.6 MHz fundamental) was attempted; and, while oscillations did occur and remain stable on the primary mode at certain EFC voltages, mode hopping was so severe during full band EFC tuning, that a 5th OT resonator (40 MHz fundamental) was then substituted. No mode hopping was experienced with the 5th OT resonator and full band data was measured. Note that the manually adjustable capacitor was not adjusted and no other components were changed aside from substituting the discrete series RLC circuit with the quartz resonator.

Similar to the previous section, Figure 6.3-1 shows the output frequency in MHz (a: blue), EFC tuning sensitivity in kHz/V (a: green), oscillator output power in dBm (b), and Vcc supply current in mA (c) all versus the EFC tuning voltage in a range from 0 to +5 V. As seen in Figure 6.3-1 and the selected data shown in Table 6.3-1, the oscillator is resonant and tunable about the desired nominal frequency of 200 MHz.

Additionally, the oscillator (now a VCXO) has an EFC bandwidth of approximately 28.6 kHz or 143 ppm[1], output power variation of less than two-tenths of a dB over the EFC band, and just over two-tenths of a mA of variation in supply current. While the tuning sensitivity is still not constant, it is again sufficient for use over small

---

[1] At 200 MHz, $1\,\text{ppm} = \frac{200\,[\text{MHz}]}{1000000} = 200\,[\text{Hz}]$. So, $28.6\,[\text{kHz}]\frac{1\,[\text{ppm}]}{200\,[\text{Hz}]} = 143\,[\text{ppm}]$.

subsets of the overall range. The 200 MHz nominal frequency occurring at an EFC voltage of approximately four volts is not ideal centering of the electrically tunable range, but adjustment of the manually tunable capacitor in the LC resonant circuit and careful varactor selection would help to better center the range about the nominal frequency.

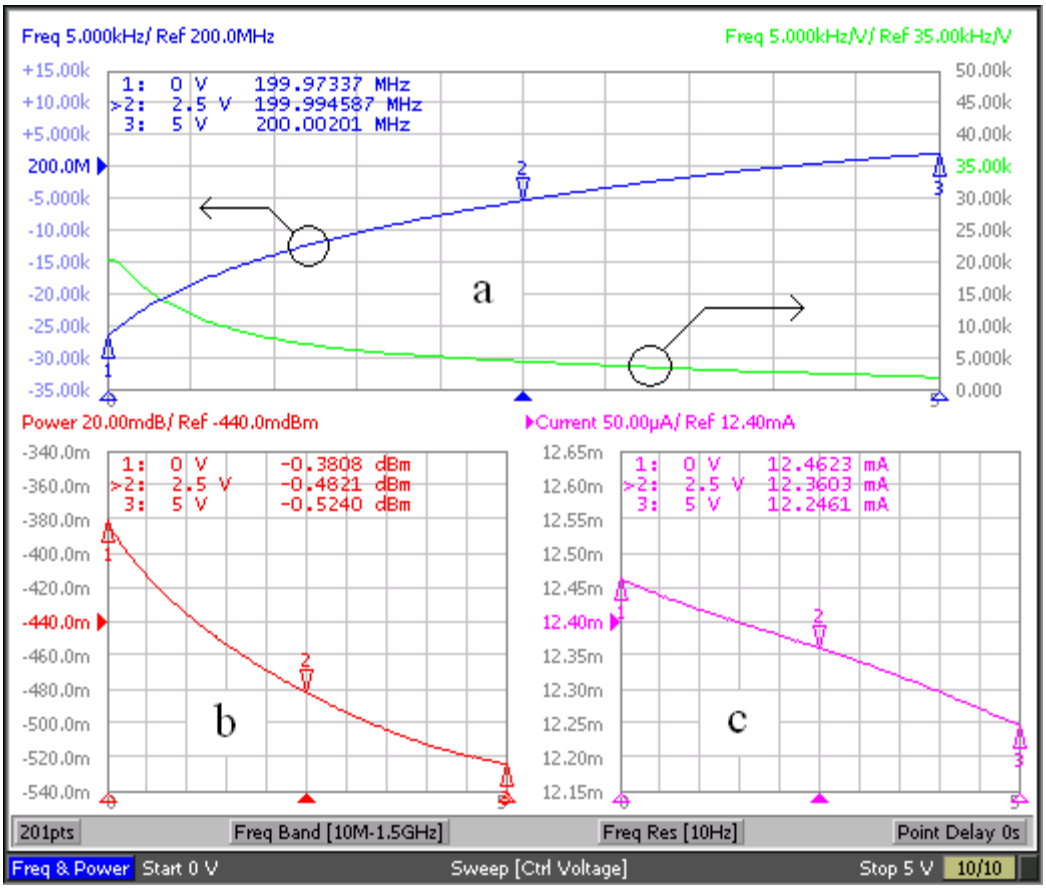

Figure 6.3-1: Swept EFC Measurements with 200 MHz 5th OT Quartz Resonator. (a: blue) Oscillator Output Frequency. (a: green) Oscillator EFC Tuning Sensitivity. (b) Oscillator Output Power. (c) Oscillator Supply Current

Table 6.3-1: SELECTED MEASURED DATA WITH 5TH OT QUARTZ RESONATOR

DC Tuning Voltage (V)	RFout (MHz)	Tuning Sensitivity (kHz/V)	Output Power (dBm)	Supply Current (mA)
0.000	199.973370	20.282	-0.381	12.462
0.500	199.981279	11.709	-0.413	12.438
1.000	199.986046	7.914	-0.436	12.417
1.500	199.989492	6.086	-0.454	12.398
2.000	199.992251	5.042	-0.469	12.379
2.500	199.994587	4.328	-0.482	12.360
3.000	199.996601	3.728	-0.494	12.340
3.500	199.998322	3.152	-0.504	12.318
4.000	199.999770	2.636	-0.513	12.295
4.500	200.000992	2.303	-0.519	12.271
5.000	200.002010	1.859	-0.524	12.246

Once again, the phase noise was also measured with the EFC voltage set to a fixed 2.5 V and is shown in Figure 6.3-2. Just as before in Figure 6.2-2, the phase noise is seen to decrease with increasing frequency offset. This time, however, it is seen to reach an intermediate floor that extends from just above 10 kHz to just above 1 MHz offset from the carrier frequency of the oscillator. The E5052A again calculated the time jitter by integrating the phase noise shown in Figure 6.3-2 using methods similar to those described in references [17, 8, and 12]. The result was approximately 2.21 ps. For Figures 6.2-2 and 6.3-2, five measurements were averaged to produce the shown plots. This helps to reduce measurement to measurement noise inherent in such a sensitive process as phase noise measurement.

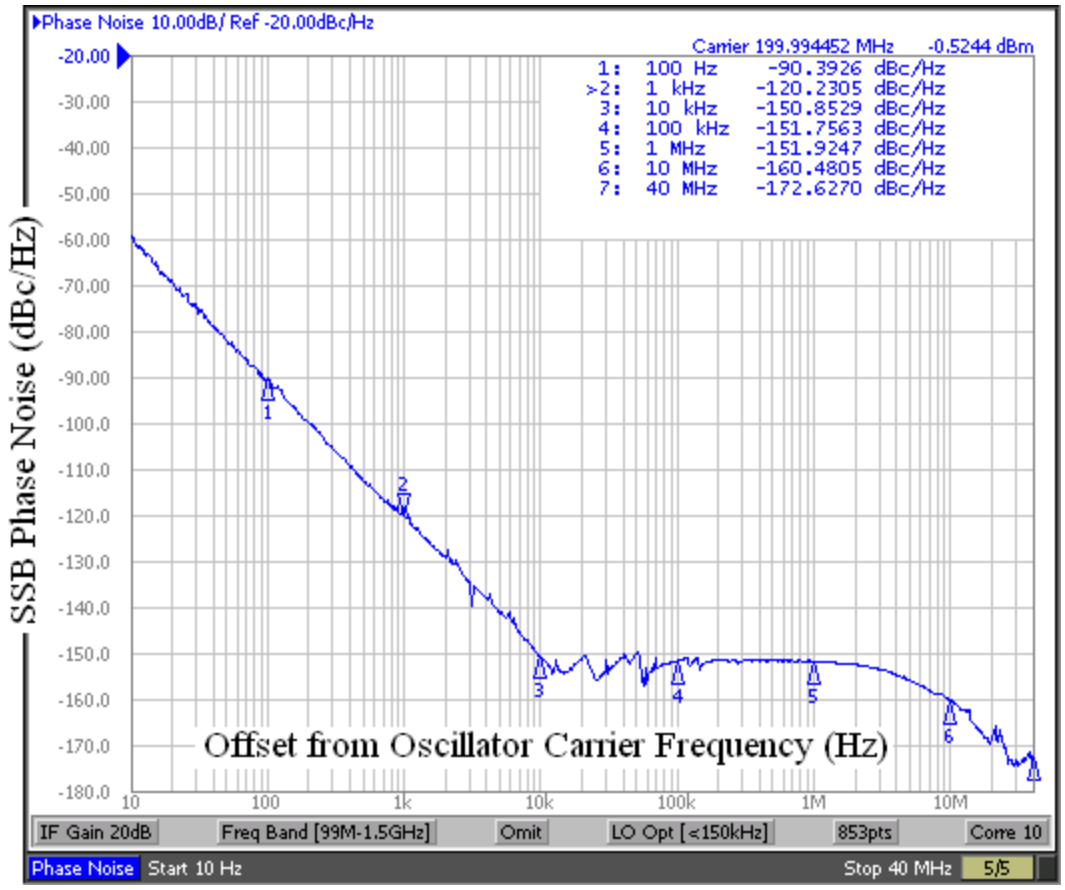

Figure 6.3-2: E5052A Phase Noise Measurement with 200MHz 5th OT Quartz Resonator

6.4 Performance Comparison of Quartz and Series RLC Oscillators

As mentioned at the beginning of this chapter, a careful comparison of the measurements will clearly illustrate the advantages and disadvantages of the quartz resonator based oscillator versus a series discrete RLC circuit. First, it is necessary to calculate the various Q factors for the series RLC circuit. This is shown in Table 6.4-1 and uses equations 4.2.1-3, 4.2.1-4, and 4.2.1-5 for Q_A, Q_B, and Q_C respectively. Note that the Q factor of the discrete series RLC resonator is much lower due to the real component values used compared to the equivalent motional values of the quartz resonator.

Table 6.4-1: COMPARISON OF Q FOR RESONATOR TYPES

Fs (MHz)	Resonator Type	$R_1(\Omega)$	C_1(fF)	L_1(mH)	Q_A	Q_B	Q_C
200.000000	Discrete Series RLC	10.0	22000	0.000027	3.62	3.39	3.50
200.000000	5th OT Quartz	11.6	0.63	1.0	108891	108331	108610

The E5052 measured EFC bandwidths for the two resonator types is summarized in Table 6.4-2. From this, it is extremely clear that using the 5th OT quartz resonator reduces the EFC bandwidth by a factor of nearly 500 compared to the discrete RLC resonator. This illustrates the claim in section 3.5.2 that stated that higher Q oscillators will have less bandwidth than lower Q oscillators and also connects with equation 3.5.1-3 that defines Q and bandwidth BW as inversely proportional for a given resonant frequency. Note the bandwidth BW referred to in equation 3.5.1-3 is the half-power bandwidth of the resonator and is proportional to, but different than, the absolute EFC tuning bandwidth measured here. The EFC tuning bandwidth is more indicative of the variable capacitive loading from the varactor pulling the series resonant frequency of the quartz resonator as described in equation 4.2.2-3.

Table 6.4-2: COMPARISON OF EFC BANDWIDTH BY RESONATOR TYPE

Fs (MHz)	Resonator Type	EFC Bandwidth (kHz)	EFC Bandwidth (ppm)
200.000000	Discrete Series RLC	13506	67530.5
200.000000	5th OT Quartz	28.64	143.2

Finally, a comparison of the phase noise performance is particularly relevant to the current work. Section 3.5.2 stated that high Q oscillators will produce less phase noise than low Q oscillators. Figure 6.4-1 shows the same phase noise plots from Figures 6.2-2 and 6.3-2 for the discrete series RLC resonator and the 5th OT quartz resonator

respectively. It is evident that the quartz resonator produces approximately 55 dB less phase noise at offsets less than 10 kHz. Above 10 kHz, the flat phase noise of the quartz resonator based oscillator allows the series RLC phase noise to catch up. They meet and are coincident from approximately 5 MHz on. This supports the earlier claims that the phase noise and the Q of the resonator are related.

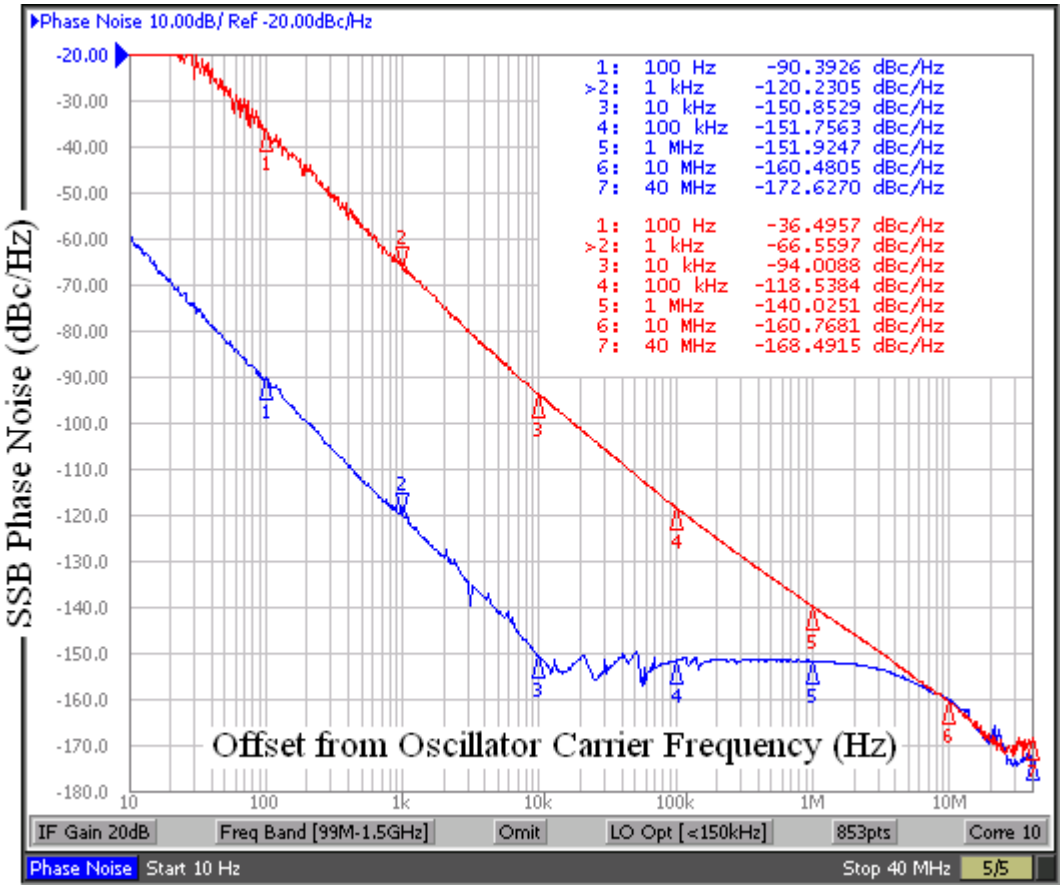

Figure 6.4-1: E5052A Phase Noise Composite of 200 MHz Quartz and Series RLC Resonators

Therefore, the claims in section 3.5.2 that the oscillator Q is both inversely proportional to bandwidth and directly proportional to phase noise performance are strongly supported by the two cases considered in this chapter. In addition to supporting

the prior claims, the comparison of the time jitter demonstrates how much more uncertain the instantaneous rising edge is per cycle with the series RLC resonator at 1330 ps versus the 5th OT quartz resonator at approximately 2.21 ps. Using equation 2.3-2, for any given analog input frequency, the magnitude of the signal to noise ratio of an ADC would be improved by 55.8 dB if a 1330 ps time jitter sample clock were replaced with a 2.21 ps time jitter sample clock. Alternately stated, a reduction in the uncertainty of the exact time that an ADC's measurements can be taken from 1330 ps to 2.21 ps represents a significant improvement in measurement accuracy. These comparisons clearly exemplify why the low jitter quartz-based oscillator is extensively used in ADC sample clocks.

Conversely, in an application where bandwidth is the primary concern and phase noise and time jitter are secondary or tertiary considerations, an oscillator using a lower Q resonator would be preferable. Another disadvantage of the quartz-based oscillator in comparison to one based on discrete RLC components is cost. A high quality quartz resonator (one manufactured to tight frequency tolerance and with well-mitigated spurious modes) could cost between $75 and $125 in small quantities while a discrete RLC circuit would likely cost much less than $1 in small quantities.

6.5 Summary of Resonator Substitution and Oscillator Retuning

In this chapter, the Two-Transistor Butler Oscillator was retuned to a frequency range near the edge of that which is attainable using traditionally manufactured quartz resonators. Measured data also reiterated the aforementioned advantages of the quartz resonator. The next step will be to substitute an inverted-mesa etched quartz resonator into the oscillator and confirm operation and performance.

CHAPTER 7
IMPLEMENTING THE 3rd OT INVERTED-MESA ETCHED QUARTZ RESONATOR

7.1 Introduction

Conversion from a traditionally manufactured 5th OT quartz resonator to a 3rd OT inverted-mesa etched quartz resonator at 200 MHz does not directly further the overall goal of extending the frequency range of the quartz-based oscillator, but it is a necessary step in the controlled evolution towards this goal. Note that the 3rd OT at 200 MHz means that the fundamental mode is approximately 67 MHz – well above the general limit of 45 MHz using traditional processing methods that require the entire quartz sample to be the same thickness. A conversion to the 3rd OT inverted-mesa etched quartz resonator and successful oscillations in the circuit without significantly degraded performance (particularly phase noise performance), would allow progression to higher frequency quartz resonators that are only possible using inverted-mesa processing.

7.2 Motional Parameter Comparison

Before substituting the resonator, it is prudent to compare the motional parameters of the 5th OT quartz resonator used in the previous chapter and the 3rd OT inverted-mesa etched quartz resonator to be used. This comparison is a valuable opportunity to make sure that the motional parameters are not so significantly different that problems should be expected. Table 7.2-1 shows that the parameters are indeed comparable.

Table 7.2-1: COMPARISON OF MOTIONAL PARAMETERS & Q

Fs (MHz)	Resonator Type	C_0 (pF)	$R_1(\Omega)$	C_1(fF)	L_1(mH)	Q_A	Q_B	Q_C
200	5th OT Quartz	2.2	11.6	0.63	1.0	108891	108331	108610
200	3rd OT Quartz	3.5	5.2	0.70	0.9	218619	217495	218056

7.3 Substitution & Measurements Using Inverted-Mesa Resonator

With the motional parameters sufficiently similar, the 3rd OT inverted-mesa etched quartz resonator is now substituted into the oscillator circuit in place of the 5th OT traditionally manufactured quartz resonator. No other changes are implemented aside from the resonator.

Upon connection to the E5052A, the circuit does indeed build up stable oscillations at and around the nominal frequency of 200 MHz over the standard EFC tuning range. Therefore, the experiment of substituting an inverted-mesa etched quartz resonator into an oscillator circuit designed for use with traditionally manufactured quartz resonators is considered successful. This result suggests that other oscillator circuits used with traditional quartz resonators should be able to accommodate inverted-mesa etched quartz resonators as well without significant alterations. However, a method of exchange at like frequencies similar to what was accomplished here is still recommended with other oscillator circuits in order to reduce unexpected and misleading failures caused by retuning the oscillator and changing quartz resonator type in the same step. Once oscillation has been successfully achieved using the inverted-mesa etched resonator, the frequencies can be increased and the oscillator circuit retuned to truly take advantage of the frequency ranges afforded by the inverted-mesa processing.

Now, the E5052A swept EFC tuning was again performed as in sections 6.2 and 6.3 and the results are displayed in Figure 7.3-1 and Table 7.3-1. The EFC bandwidth of the VCXO is approximately 24.6 kHz or 123 ppm, output power variation is less than one-tenth of a dB over the EFC band, and less than two-tenths of a mA of variation is obtained in supply current. The tuning sensitivity shows a similar trend as in Figure 6.3-2 and is somewhat jagged because the measurement resolution is 1 kHz rather than 10 Hz.

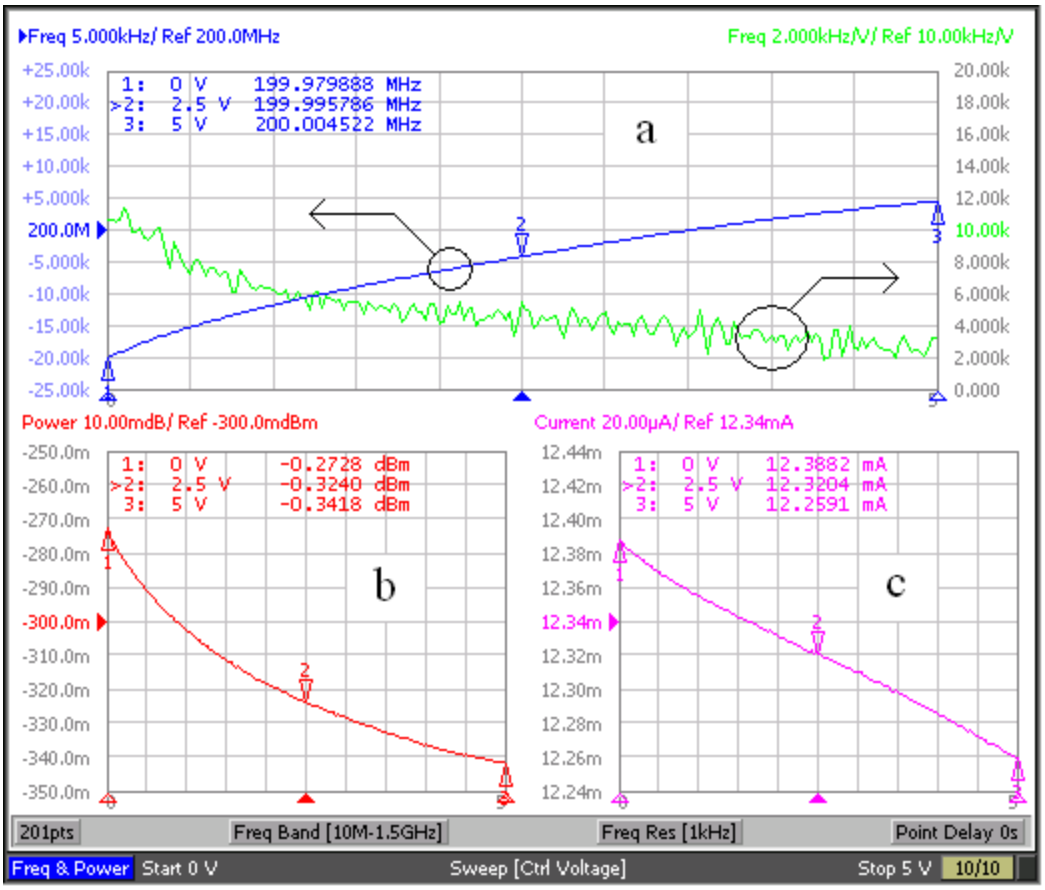

Figure 7.3-1: Swept EFC Measurements with 200 MHz 3rd OT Inverted-Mesa Quartz Resonator. (a: blue) Oscillator Output Frequency. (a: green) Oscillator EFC Tuning Sensitivity. (b) Oscillator Output Power. (c) Oscillator Supply Current

Table 7.3-1: SELECTED MEASURED DATA WITH 3RD OVERTONE QUARTZ RESONATOR

DC Tuning Voltage (V)	RFout (MHz)	Tuning Sensitivity (kHz/V)	Output Power (dBm)	Supply Current (mA)
0.00	199.979888	10.673	-0.273	12.388
0.50	199.984659	7.199	-0.291	12.369
1.00	199.988159	6.256	-0.302	12.355
1.50	199.990982	5.472	-0.311	12.342
2.00	199.993488	4.149	-0.318	12.331
2.50	199.995786	5.416	-0.324	12.320
3.00	199.997971	4.894	-0.328	12.310
3.50	199.999900	3.178	-0.333	12.298
4.00	200.001664	3.390	-0.336	12.285
4.50	200.003210	2.616	-0.339	12.272
5.00	200.004522	3.170	-0.342	12.259

Again, as in sections 6.2 and 6.3, the phase noise was measured at a fixed EFC voltage of 2.5 volts and is shown below in Figure 7.3-2. The E5052A calculated time jitter from the phase noise shown in Figure 7.3-2 is approximately 2.15 ps. As before, five measurements were averaged to produce the plot in Figure 7.3-2.

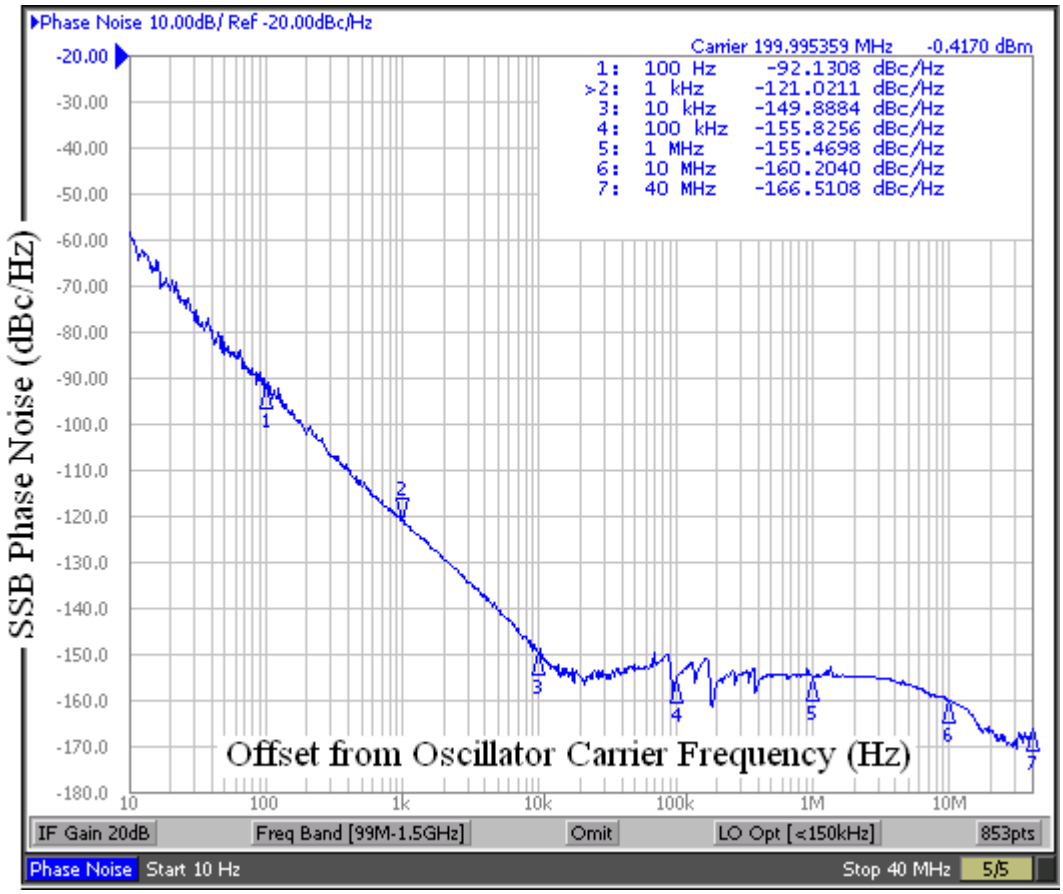

Figure 7.3-2: E5052A Phase Noise Measurement with 200 MHz 3rd OT Inverted-Mesa Quartz Resonator

7.4 Performance Comparisons with 5th OT Traditional Resonator

Now that oscillations have been confirmed and characterized, it is important to ensure that no significant degradation in performance occurred when the oscillator was changed from the 5th OT traditionally manufactured quartz resonator to the 3rd OT inverted-mesa etched quartz resonator. In Table 7.4-1, swept EFC tuning measurements are summarized from sections 6.3 and 7.3. This side-by-side comparison shows that the exchange of the two quartz resonator types did not significantly alter the output power or the supply current over the EFC range. The EFC tuning bandwidth is seen to decrease by approximately 15% with the substitution of the 3rd OT inverted-mesa resonator.

The capacitance ratio r and the %BW first introduced in section 4.2.2 are also shown in Table 7.4-1 and confirm that a decrease should be seen in the bandwidth achieved by the two oscillators if all other contributing factors remain unchanged. Since nothing was changed except the quartz resonator between measurements, the decreases in the EFC BW and the %BW are in excellent agreement. Note that the amount of the decreases do not need to agree or even be similar since the EFC BW is mostly controlled by the capacitance range of the varactor and the %BW is calculated strictly based on the motional parameters of the resonator.

Table 7.4-1: EFC SWEEP MEASUREMENT & BW COMPARISONS

Resonator Type	200 MHz 5th OT Quartz	200 MHz 3rd OT Quartz
Manufacturing	Traditional	Inverted-Mesa Etched
Power Range (dBm)	-0.3808 to -0.5240	-0.2728 to -0.3418
Icc Range (mA)	12.4623 to 12.2461	12.3882 to 12.2591
EFC Range (V)	0 to +5	0 to +5
EFC BW (kHz)	28.64	24.63
EFC BW (ppm)	143.2	123.2
EFC BW Normalized	1	0.860335
r	3492	5000
%BW	0.014355	0.010026
%BW Normalized	1	0.698433

Next, the phase noise measurements will be compared to ensure that degradation in this critical aspect of performance was not introduced. As before, the most effective method of comparison is to superpose the two phase noise measurement plots in the same figure – this is shown in Figure 7.4-1. Below offset frequencies of 10 kHz, the phase noise of the two oscillators is nearly identical. Above this point, there is some slight variation, but the comparison clearly shows that the phase noise was not significantly degraded upon substitution of the new resonator type.

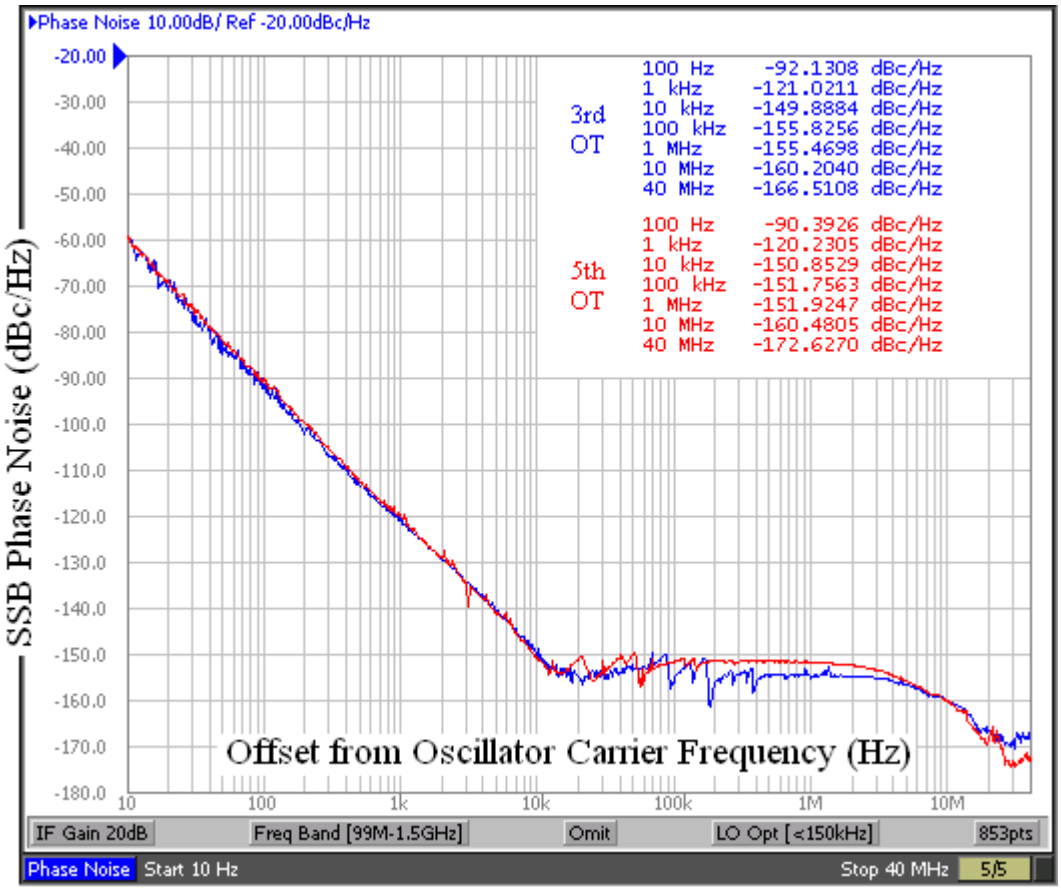

Figure 7.4-1: E5052A Phase Noise Composite of 200 MHz 5th OT Traditional and 3rd OT Inverted-Mesa Quartz Resonators

7.5 Conclusions from Inverted-Mesa Etched Resonator Substitution

This chapter included the direct substitution of a 3rd OT inverted-mesa etched quartz resonator for a 5th OT traditionally manufactured quartz resonator in an OT oscillator tuned to operate at a nominal frequency of 200 MHz. The oscillator successfully operated under the control of the inverted-mesa resonator and was shown to produce very similar EFC characteristics and phase noise. Based on this success, as already stated, it is logical to expect that other OT oscillator circuits should be capable of operating with inverted-mesa etched quartz resonators. Naturally, an incremental process of retuning followed by substitution similar to that accomplished in chapters 6 and 7 above is recommended to reduce confusion and potential failure due to compounding the retuning and substitution steps.

Once performance has been confirmed using the inverted-mesa etched quartz resonators, as it has been here, the retuning step can be repeated to further increase the frequency of the oscillator to one that takes better advantage of the higher range afforded by the inverted-mesa quartz resonators. This step will be performed in the next chapter to produce an oscillator whose nominal frequency would not be possible using a traditionally manufactured quartz resonator.

CHAPTER 8
RETUNING TO A 356.875 MHZ 3RD OT INVERTED-MESA RESONATOR

8.1 Introduction

This chapter directly furthers the overall goal of extending the frequency range of the quartz-based oscillator by retuning the oscillator circuit for a 3rd OT 356.875 MHz inverted-mesa etched quartz resonator. The 3rd OT at 356.875 MHz means that the fundamental mode is resonant at approximately 120 MHz which is nearly three times the general limit of 45 MHz using traditional cutting and grinding methods. This truly represents a situation that would not be possible without the inverted-mesa processing.

8.2 Retuning Summary and Oscillator Measurements

The method introduced in chapter 6 will be used to retune the oscillator. In addition to retuning the second LC resonant circuit (the OT selection circuit), this frequency change required new transistors capable of higher frequency operation, a new higher-Q type of manually adjustable capacitor, and a new varactor with a different range of reverse-biased junction capacitance. Once stable at the new nominal frequency, the inverted-mesa quartz resonator described by the equivalent circuit motional parameters shown in Table 8.2-1 was installed into the Two-Transistor Butler Oscillator. In addition to the motional parameters of the resonator, Table 8.2-1 also shows some other figures of merit that have been discussed in previous chapters and found to be useful in the analysis of the oscillator measurements and comparisons – such as Q, r, and %BW. Once the oscillator was under the control of the new quartz resonator, swept EFC tuning measurements were taken as in prior cases and are shown in Figure 8.2-1.

Table 8.2-1: EQUIVALENT CIRCUIT VALUES & CALCULATED FIGURES OF MERIT FOR 356.875 MHZ 3RD OT INVERTED-MESA ETCHED QUARTZ RESONATOR

F_{nom} (MHz)	356.875000
Resonator Mode	3rd OT
C_0(pF)	2.975
$R_1(\Omega)$	29.3
C_1(fF)	0.53
L_1(mH)	0.373635
Q_A	28718
Q_B	28594
Q_C	28656
r	5613
f_s (Hz)	357650158
f_a (Hz)	357682016
% BW	0.008927

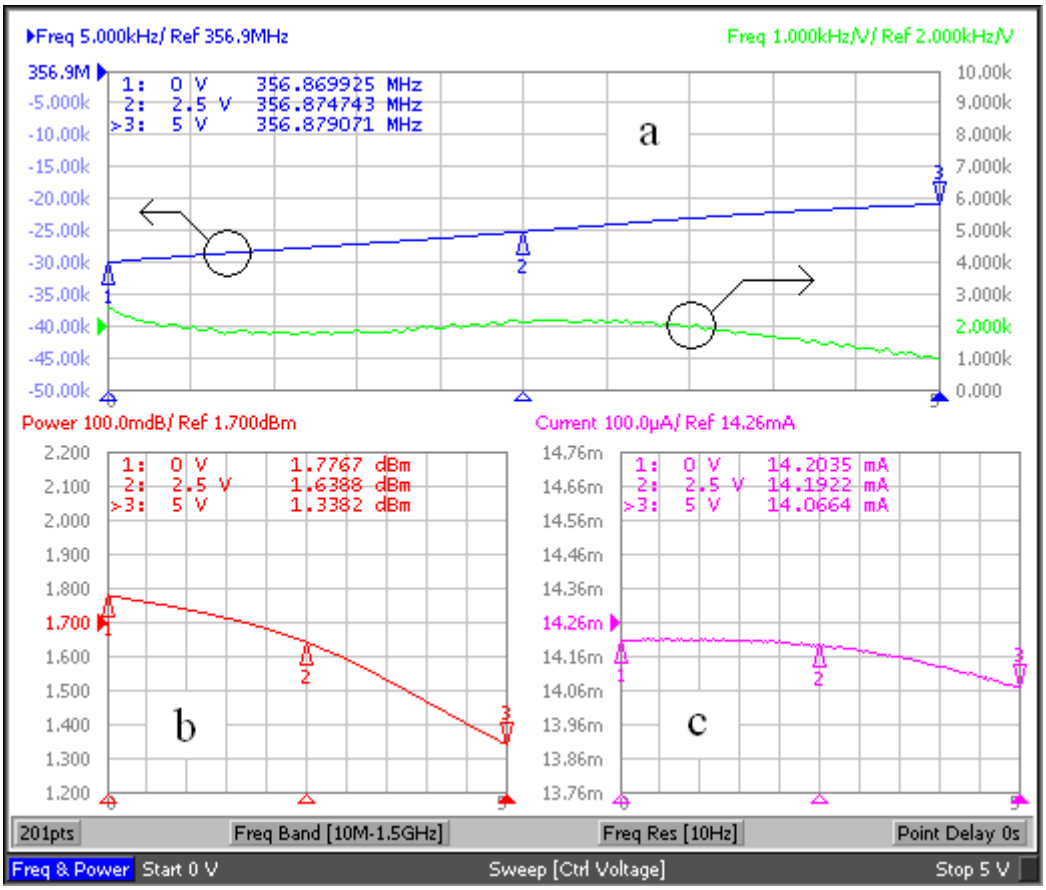

Figure 8.2-1: Swept EFC Measurements with 356.875 MHz 3rd OT Inverted-Mesa Quartz Resonator. (a: blue) Oscillator Output Frequency. (a: green) Oscillator EFC Tuning Sensitivity. (b) Oscillator Output Power. (c) Oscillator Supply Current

The swept EFC data shows that the EFC bandwidth of the new 356.875 MHz VCXO is approximately 9.15 kHz or 25.6 ppm, output power variation is less than one-half of a dB over the EFC band, and less than two-tenths of a mA of variation is obtained in supply current. The tuning sensitivity and the EFC bandwidth shown in Figure 8.2-1 are significantly different from those in previous chapters due to the circuit changes above – particularly the change of the varactor. Again, the phase noise was measured with the EFC voltage set to 2.5 volts and is shown in Figure 8.2-2. The E5052A calculated time jitter is 0.824 ps.

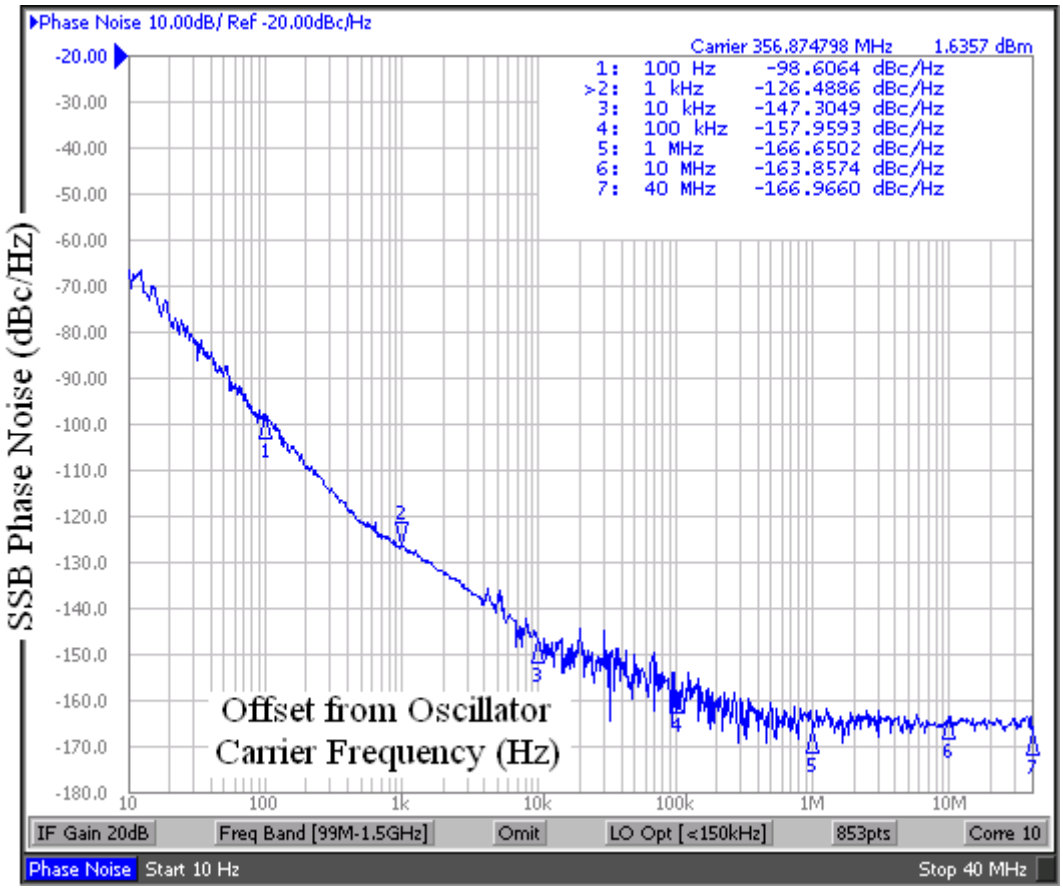

Figure 8.2-2: E5052A Phase Noise Measurement of 356.875 MHz 3rd OT Inverted-Mesa Etched Quartz Resonator Based VCXO

8.3 Discussion of Measured Results

Due to the considerable changes in the oscillator circuit mentioned in the previous section and the significantly higher frequency, direct comparisons of specific measured data with that of prior chapters is not objective. However, it is useful to note that the general performance was very similar to the 200 MHz VCXO in the previous chapter. The largest difference in performance was the reduced EFC bandwidth due in large part to the varactor having been changed. The second most notable difference is the general trend of the tuning sensitivity. In all previous oscillators measured, the tuning sensitivity displayed significantly non-linear trends across the EFC tuning range. Figure 8.2-1 shows a tuning sensitivity with a nearly linear trend over most of the tuning range. From EFC near 0 V to approximately +4 V, the tuning sensitivity remains within very tight tolerance of approximately 2 kHz/V. This is also mostly due to the change in varactor and is a benefit – especially considering that the EFC bandwidth itself was so reduced.

Also note that the phase noise performance was nearly as good and, in fact, better at certain offsets than that measured from the 200 MHz VCXOs tested in previous chapters – as evidenced by the reduced time jitter. This is particularly useful since the output from a lower frequency crystal oscillator would have been passed through a frequency multiplier to achieve this frequency output prior to inverted-mesa processing. Frequency multipliers will increase the frequency by an integer factor, but will also increase the phase noise and jitter.

CHAPTER 9
SUMMARY & FUTURE WORK

9.1 Summary and Discussion

The thesis was introduced as an experiment to advance electronic oscillator design using inverted-mesa etched quartz resonators. The primary goal was to increase the maximum frequency range of a quartz resonator based oscillator without using an external multiplier. The motivation was that the low phase noise and low jitter inherent in these quartz resonator oscillators could be used to improve overall performance in systems that are currently phase noise or jitter limited. Two such applications that were introduced and discussed were wireless communications systems and sampled data systems. These examples represent areas where the operating frequencies are increasing to meet the demand of advancing technology and where phase noise and jitter levels in electronic oscillators introduce system performance limitations.

Considerable background was provided on electronic oscillators and quartz resonators to enable an understanding of the quartz resonator based oscillator. This included the introduction to the use of quartz as a piezoelectric material and to the equivalent electronic circuit of a quartz resonator. The practical limitations of the traditionally manufactured quartz resonator were introduced and the inverted-mesa etched quartz resonator was proposed as a potential solution.

The Two Transistor Butler Oscillator was introduced as a functioning OT quartz resonator oscillator and was described qualitatively and simulated using a commercially available software package. The oscillator was shown to function and was tuned for use at a nominal frequency of 200 MHz. The process of tuning the oscillator was described

and provided the opportunity to observe and compare the performance of the oscillator under control of a quartz resonator versus a resonator comprised of discrete RLC components.

Finally, in chapter 7, an inverted-mesa etched quartz resonator was introduced into the oscillator and was found to provide a performance comparable to a traditionally manufactured quartz resonator at 200 MHz. In chapter 8 the oscillator was again retuned, but for a nominal frequency of approximately 356 MHz. The inverted-mesa etched quartz resonator used at this frequency definitively shows that the quartz resonator can extend beyond the frequency limitations inherent in the traditional manufacturing method.

9.2 Future Work

The most significant remaining work is to measure the performance of the new inverted-mesa etched quartz resonator VCXO while exposing the oscillator to various operating environments. The performance of the oscillator over wide ambient temperature ranges is particularly important. Since the quartz resonator itself is an electromechanical transducer, operation during and after mechanical shock and vibration should also be carefully tested.

Another important aspect to be studied is the ultimate upper frequency limitations of the inverted-mesa etched quartz resonator. If not limited by upper frequency (as may be inferred by the work done in references [34] and [35]), the upper limitation may be imposed by gradual or abrupt deterioration of the achievable performance in such critical performance parameters as phase noise and jitter. Alternately, it may be found to have the same limitation as the traditionally manufactured quartz resonator – manufacturing feasibility and cost.

BIBLIOGRAPHY

[1] David M. Pozar, "Microwave and RF Design of Wireless Systems", John Wiley & Sons, Inc., New York, 2001.

[2] American National Standard ANSI/SCTE 07 2006, *Digital Transmission Standard for Cable Television*, 2006.

[3] John F. Wakerly, "Digital Design: Principles and Practices 3rd Edition," Prentice-Hall, Inc., New Jersey, 2001.

[4] Mark R. Simpson and John M. Dixon, "The Application of Low Noise X-Band Synthesizers to QAM Digital Radios," *Microwave Journal*, July 1997, pp. 76-86.

[5] Mark Kolber, "Predict Phase-Noise Effects in Digital Communications Systems," Microwaves & RF, September 1999, pp. 59-70.

[6] Kent K. Johnson, "Optimizing Link Performance, Cost and Interchangeability by Predicting Residual BER: Part I – Residual BER Overview and Phase Noise," Microwave Journal, July 2002, pp. 20-30.

[7] Adrian Fox, "Ask the Applications Engineer – 30: PLL Synthesizers," Analog Dialogue, Volume 36 – Issue 1, 2002, pp. 13-16.

[8] Brad Brannon, "Sampled Systems and the Effects of Clock Phase Noise and Jitter," Application Note AN-756 REV.0, Analog Devices, Inc., December 2004.

[9] Paul Smith, "Little Known Characteristics of Phase Noise," Application Note AN-741 REV.0, Analog Devices, Inc., August 2004.

[10] Bar-Giora Goldberg, "The Effects of Clock Jitter on Data Conversion Devices," *RF Design*, August 2002, pp. 26-32.

[11] Paul Nunn, "Reference-Clock Generation for Sampled Data Systems," *High Frequency Electronics*, September 2005, pp. 48-57.

[12] Rob Reeder, Wayne Green, and Robert Shillito, "Analog-to-Digital Converter Clock Optimization: A Test Engineering Perspective," Analog Dialogue, Volume 42 (2008) Number 1, pp. 6-12.

[13] Brad Brannon and Allen Barlow, "Aperture Uncertainty and ADC System Performance," Application Note AN-501 REV.A, Analog Devices, Inc., March 2006.

[14] Brad Brannon and Chris Cloninger, "Redefining the Role of ADCs in Wireless," *Applied Microwave & Wireless*, March 2001, pp. 94-105.

[15] Harry Nyquist, "Certain Factors Affecting Telegraph Speed," *Bell System Technical Journal*, Vol. 3, April 1924, pp. 324-346.

[16] Walt Kester, "What the Nyquist Criterion Means to Your Sampled Data System Design," Tutorial MT-002 REV.A, Analog Devices, Inc., October 2008.

[17] Walt Kester, "Converting Oscillator Phase Noise to Time Jitter," Tutorial MT-008 REV.A, Analog Devices, Inc., October 2008.

[18] David M. Pozar, "Microwave Engineering 3rd Edition," John Wiley & Sons Inc., New Jersey, 2005.

[19] Donald A. Neamen, "Microelectronics: Circuit Analysis and Design 3rd Edition," The McGraw-Hill Companies, Inc., New York, 2007.

[20] Marvin E. Frerking, "Crystal Oscillator Design and Temperature Compensation", Van Nostrand Reinhold Company, New York, 1978.

[21] Rick Cory, "The Nuts and Bolts of Tuning Varactors," *High Frequency Electronics*, February 2009, pp. 42-51.

[22] "Quartz Tech," Application Note, Fortiming Corporation, http://www.4timing.com/techquartz.htm, Accessed 5/25/2009.

[23] "Technical Glossary," Application Note, Fortiming Corporation, http://www.4timing.com/termcrystal.htm, Accessed 5/25/2009.

[24] Louis Bradshaw, "Comparing Round and Rectangular Crystals," *Microwaves & RF*, November 1999, pp. 85-92.

[25] Ken Hennessy, "Quartz Crystal Basics: From Raw Materials to Oscillators," *High Frequency Electronics*, December 2007, pp. 54-58.

[26] "Types of Crystal Cut," Application Note, Citizen Holdings Co. Ltd., http://www.citizen.co.jp/english/crystal/cut/index.html, Accessed 3/21/2009.

[27] "Quartz Crystal Theory of Operation," Application Note, Fox Electronics, 2004, http://www.foxonline.com/pdfs/xtaltheoryoper.pdf, Accessed 3/21/2009.

[28] "Crystal Technology," Application Note, Fortiming Corporation, http://www.4timing.com/techcrystal.htm, Accessed 5/25/2009.

[29] Public domain images obtained from http://en.wikipedia.org/wiki/Quartz_oscillator, Accessed 3/21/2009.

[30] "Equivalent Circuit of a Resonator," Application Note, Citizen Holdings Co. Ltd, http://www.citizen.co.jp/english/crystal/circuit/index.html, Accessed 5/25/2009.

[31] "Motional Capacitance & Motional Inductance," Application Note, Anderson Electronics Inc., http://www.aextal.com/tutorial-motional-capacitance.htm, Accessed 5/25/2009.

[32] Martin Finkelstein, "Inverted-Mesa Crystals Carry Oscillators Into the Internet Age," *Electronic Design*, March 6, 2000.

[33] Dan Nehring, "Novel High-Frequency Crystal Oscillator Cuts Jitter and Noise," *RF Design*, June 2005, pp. 32-42.

[34] H. Yamada, H. Ural, H. Fujiyama, "620 MHz AT-Cut Fundamental Crystal Resonator," *IEEE International Frequency Control Symposium and PDA Exhibition*, 2002, pp. 174-178.

[35] Hirokazu Iwata, "Measured Resonance Characteristics of a 2-GHz-Fundamental Quartz Resonator," *IEEE Transactions on Ultrasonics, Ferroelectrics, and Frequency Control*, vol. 51, no. 8, pp. 1026-1029, August 2004.

[36] Benjamin Parzen and Arthur Ballato, "Design of Crystal and Other Harmonic Oscillators," John Wiley & Sons Inc., November 1982.

[37] Robert J. Matthys, "Crystal Oscillator Circuits, Revised Edition," Krieger Publishing Company, Florida, April 1991.